

EXPLORING THE IMF WITH N_2H^+ : MORPHOLOGICAL ANALYSIS OF THE G327.29 PROTOCLUSTER.



Universidad de los Andes | Physics Department
COCOA- Bucaramanga | Nov 20 | 2024



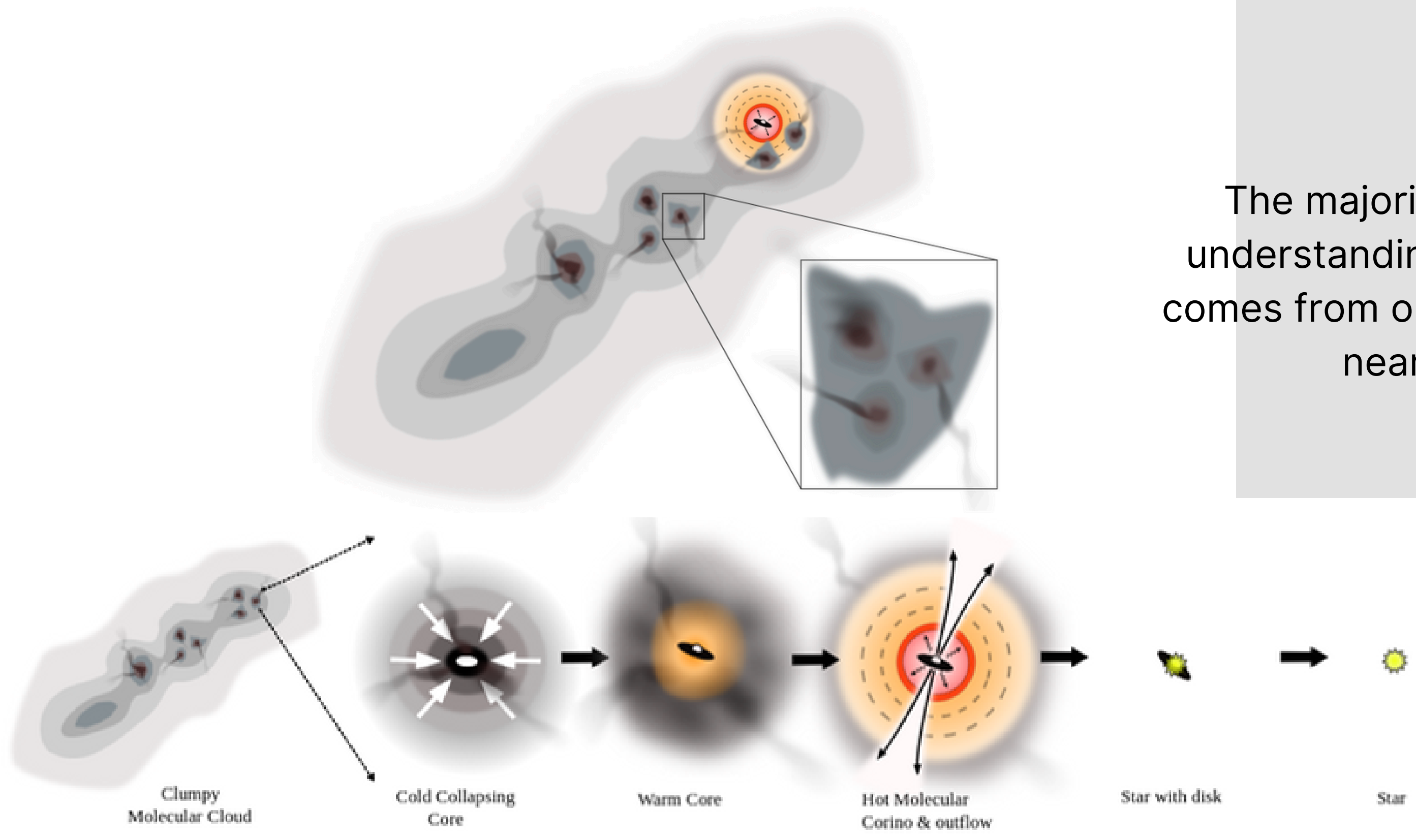
Presentation by **Fredy Orjuela**
Advisor **PhD Beatriz Sabogal**

OVERVIEW

- 01 Star-Forming Regions**
- 02 Initial Mass Function**
- 03 ALMA - G327.29**
- 04 Methodology N₂H⁺**
- 05 Conclusions**

Star-Forming Regions

LOW MASS STAR FORMATION



The majority of our detailed understanding of star formation comes from observations of small, nearby clouds.

Figure 1. Ginsburg, A. (2024)

HIGH MASS STAR FORMATION

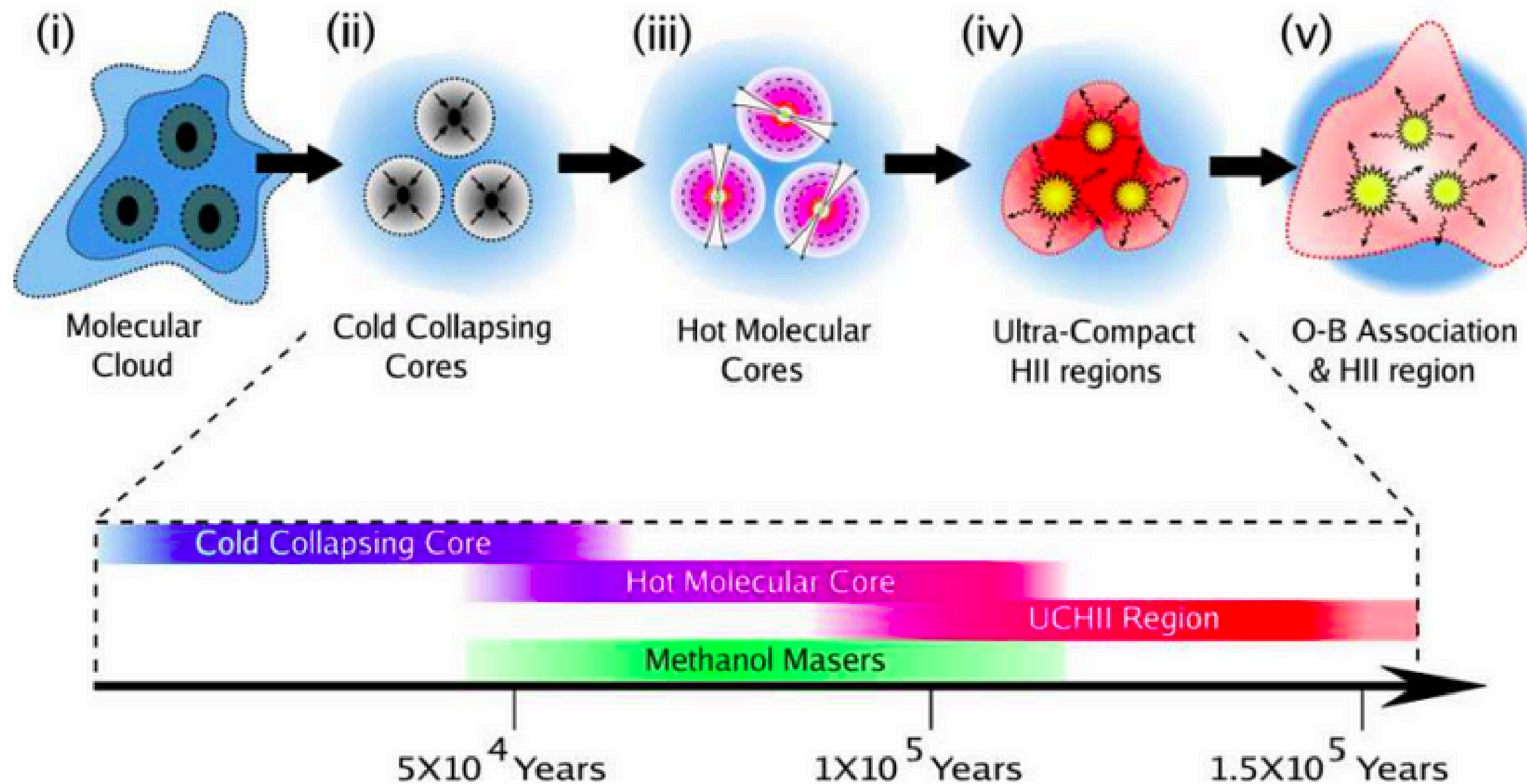


Figure 2. Purcell, C. (2006)

Massive Star
Formation

Collapse and Mass
Increase

Complex
Hydrocarbon
Creation

Ultra-Compact HII
Regions

Expansion of HII
Region and Cluster
Exposure

Initial Mass Function

INITIAL MASS FUNCTION

$$\phi(M)dM \simeq 0.584M_{\odot}^{-1} \exp \left\{ -1.54 \log^2 \left[\frac{M}{0.22M_{\odot}} \right] \right\} \frac{dM}{M}$$

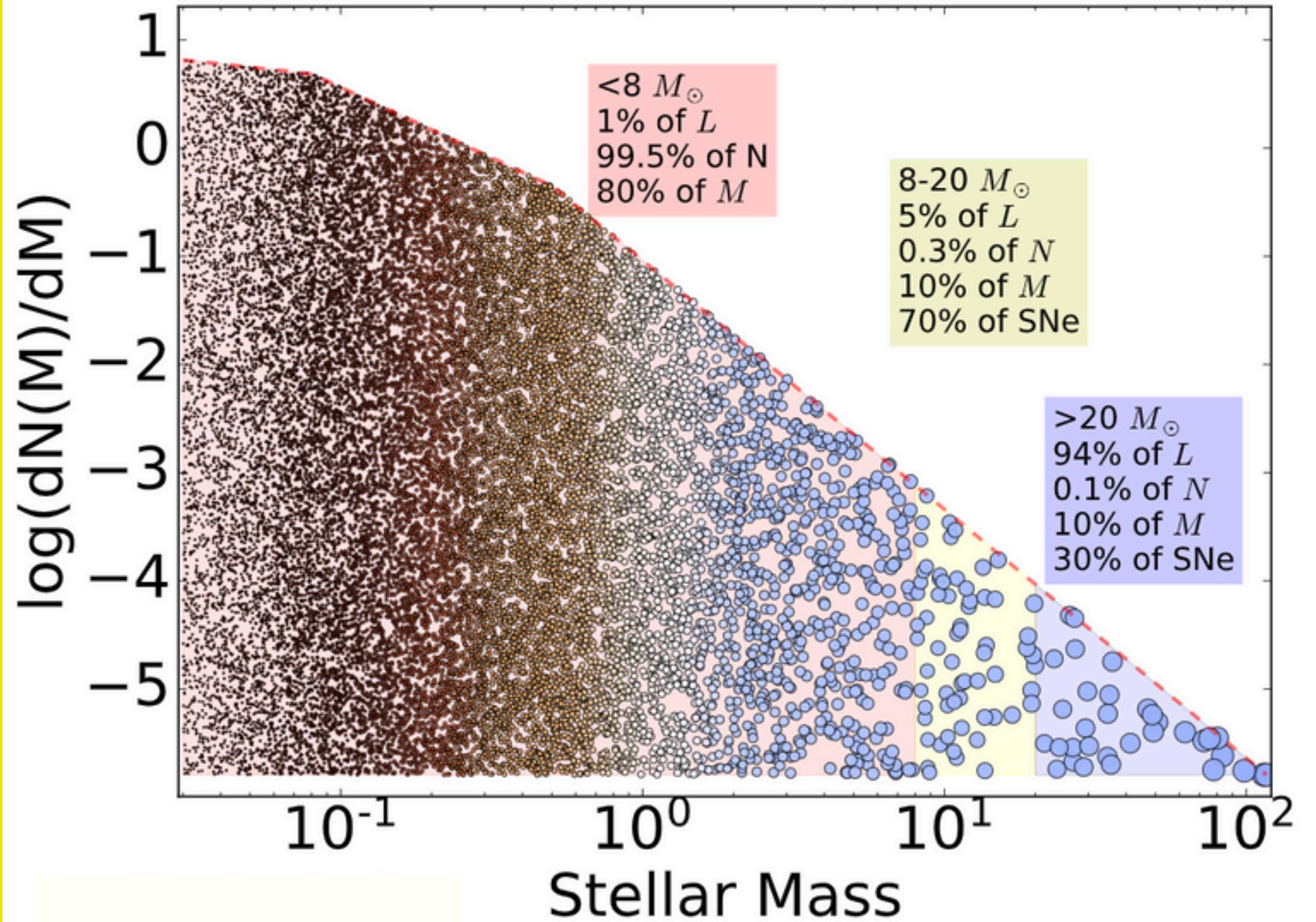
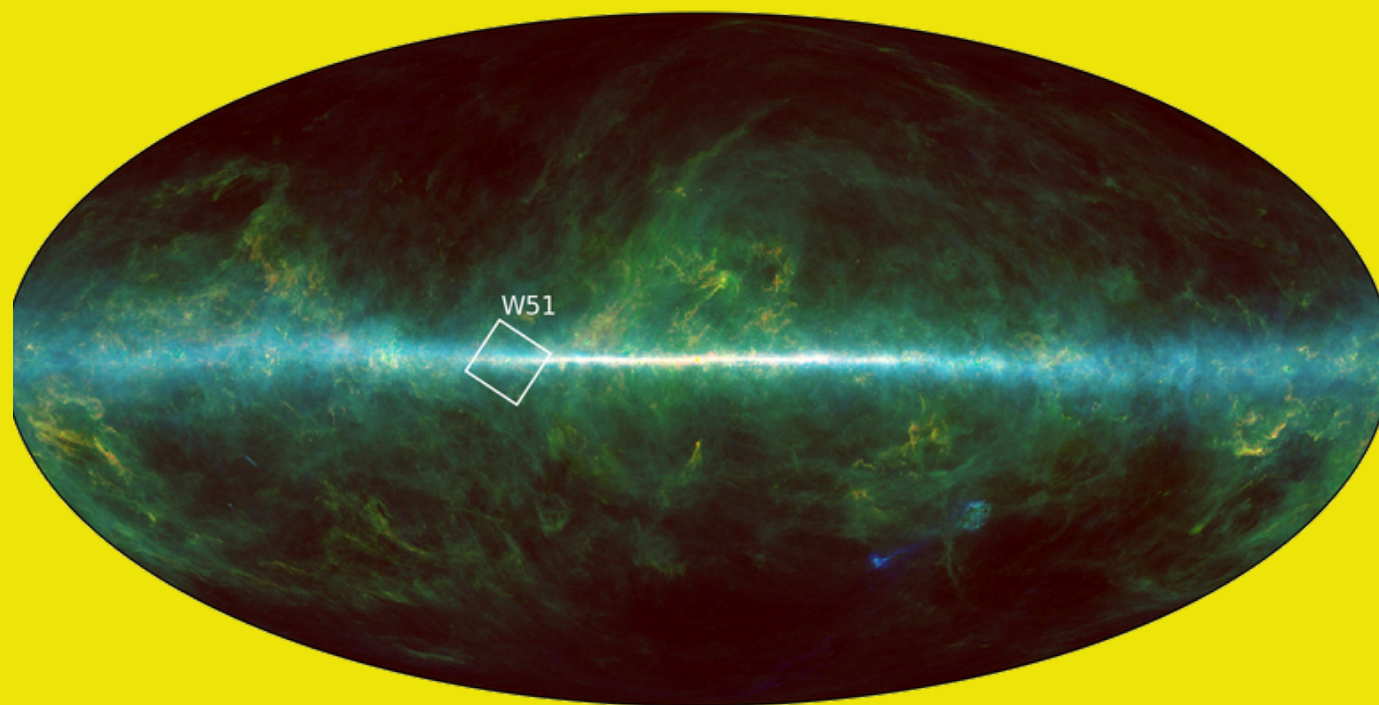
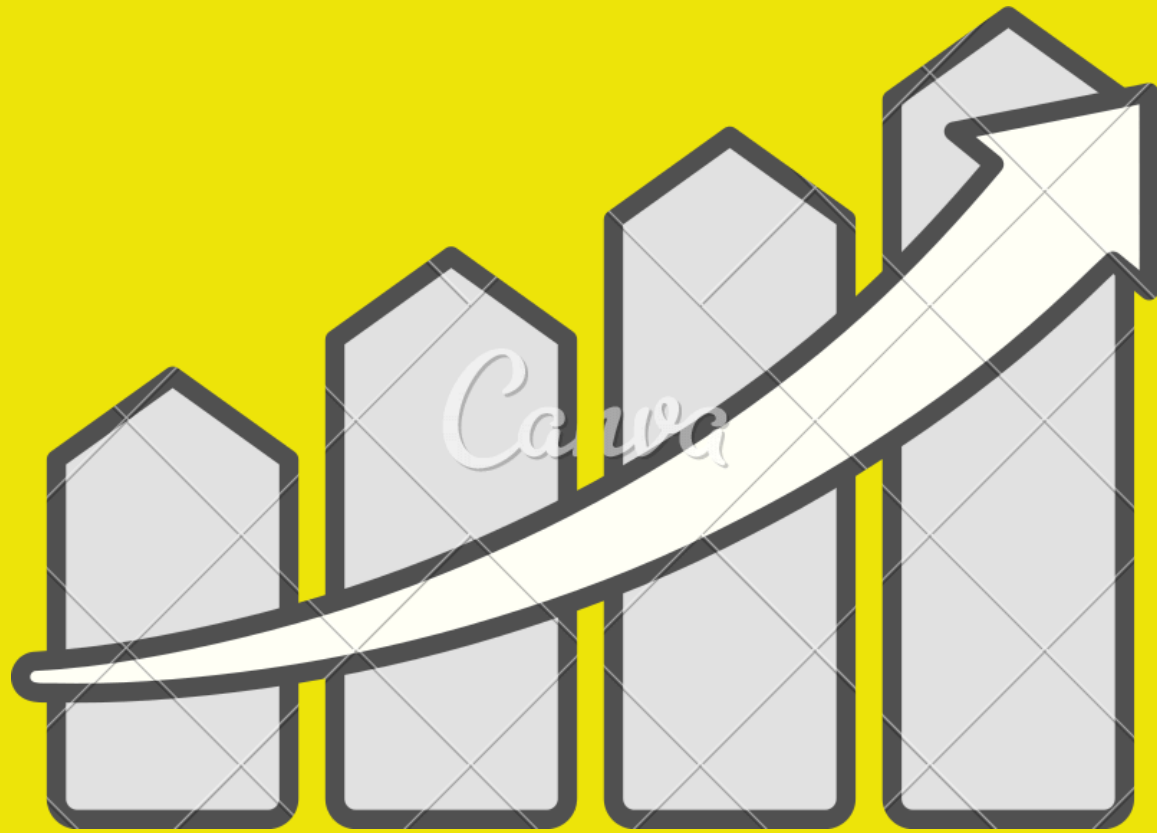


Figure 3. Ginsburg, A. (2024)

PROPOSED/FUTURE TELESCOPES

1. How does the IMF (initial mass function) change, and what controls its changes?
2. What controls the rate of star formation in galaxies?
3. When and how do planets form?
4. How does the grouping of stars affect each of these processes?

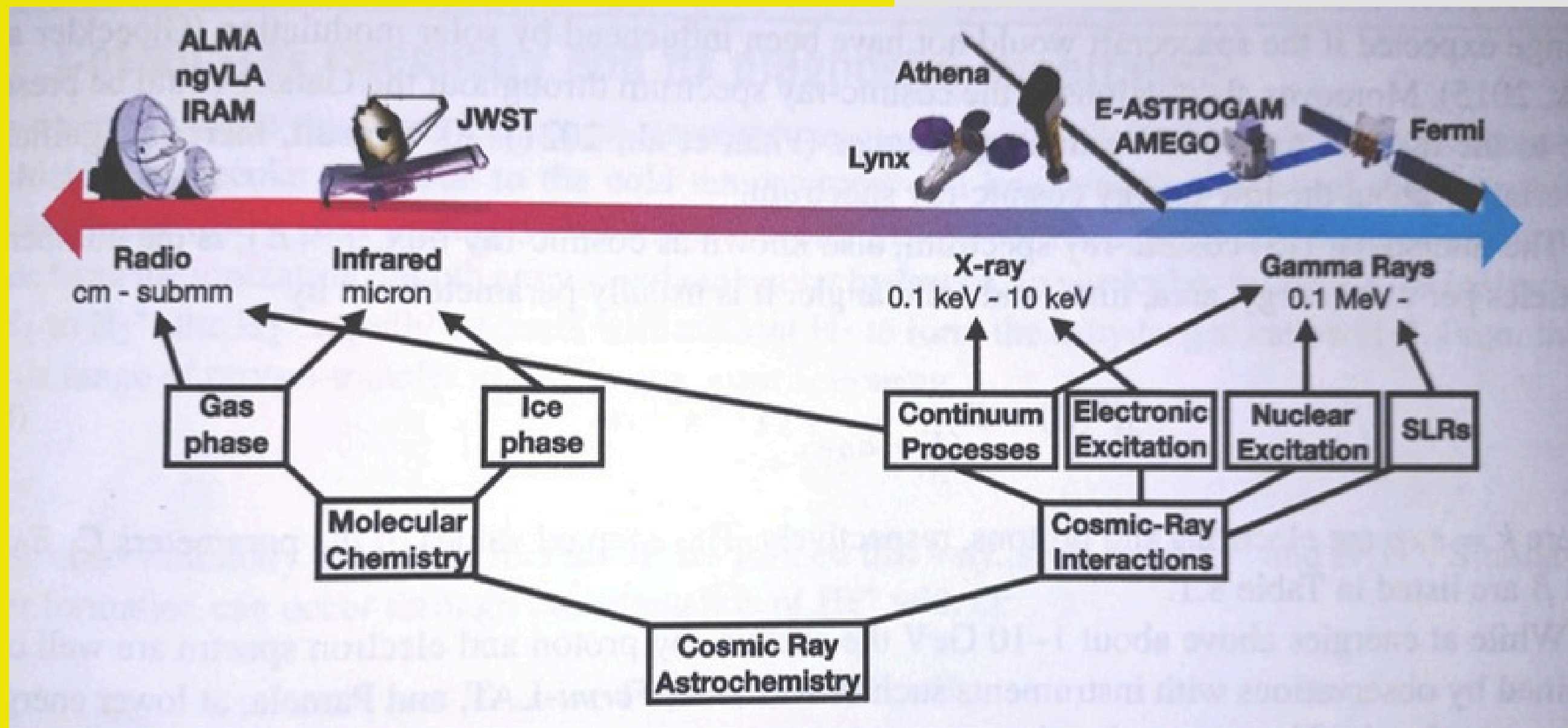



Figure 4. Bovino, S. (2024)

ALMA IMF - G327.29

ALMA IMF LARGE PROGRAM

ALMA-IMF

I. Investigating the origin of stellar masses: Introduction to the Large Program and first results

F. Motte¹ , S. Bontemps², T. Csengeri², Y. Pouteau¹, F. Louvet^{1,3,4}, A. M. Stutz^{5,6}, N. Cunningham¹, A. López-Sepulcre^{1,7}, N. Brouillet², R. Galván-Madrid⁸, A. Ginsburg⁹, L. Maud¹⁰, A. Men'shchikov³, F. Nakamura^{11,12,13}, T. Nony⁸, P. Sanhueza^{11,12}, R. H. Álvarez-Gutiérrez⁵, M. Armante^{14,15}, T. Baug¹⁶, M. Bonfand², G. Busquet^{1,17,18}, E. Chapillon^{2,7}, D. Díaz-González⁸, M. Fernández-López¹⁹, A. E. Guzmán¹¹, F. Herpin², H.-L. Liu^{5,20}, F. Olguin²¹, A. P. M. Towner⁹, J. Bally²², C. Battersby²³, J. Braine², L. Bronfman²⁴, H.-R. V. Chen²¹, P. Dell'Ova¹⁴, J. Di Francesco²⁵, M. González³, A. Gusdorf¹⁴, P. Hennebelle³, N. Izumi^{11,26,27}, I. Joncour¹, Y.-N. Lee²⁸, B. Lefloch¹, P. Lesaffre¹⁴, X. Lu¹¹, K. M. Menten²⁹, R. Mignon-Risse³, J. Molet², E. Moraux¹, L. Mundy³⁰, Q. Nguyễn Lương³¹, N. Reyes^{29,32}, S. D. Reyes Reyes⁵, J.-F. Robitaille¹, E. Rosolowsky³³, N. A. Sandoval-Garrido⁵, F. Schuller^{29,34}, B. Svoboda³⁵, K. Tatematsu¹¹, B. Thomasson¹, D. Walker³⁶, B. Wu^{11,37}, A. P. Whitworth³⁸, and F. Wyrowski²⁹



F.Motte



A.M. Stutz

Mass Stars

How is the
Formation?

Parameter
es

Variety in
Size and
Temp

Importance
in the
Universe

STAR-FORMING REGIONS

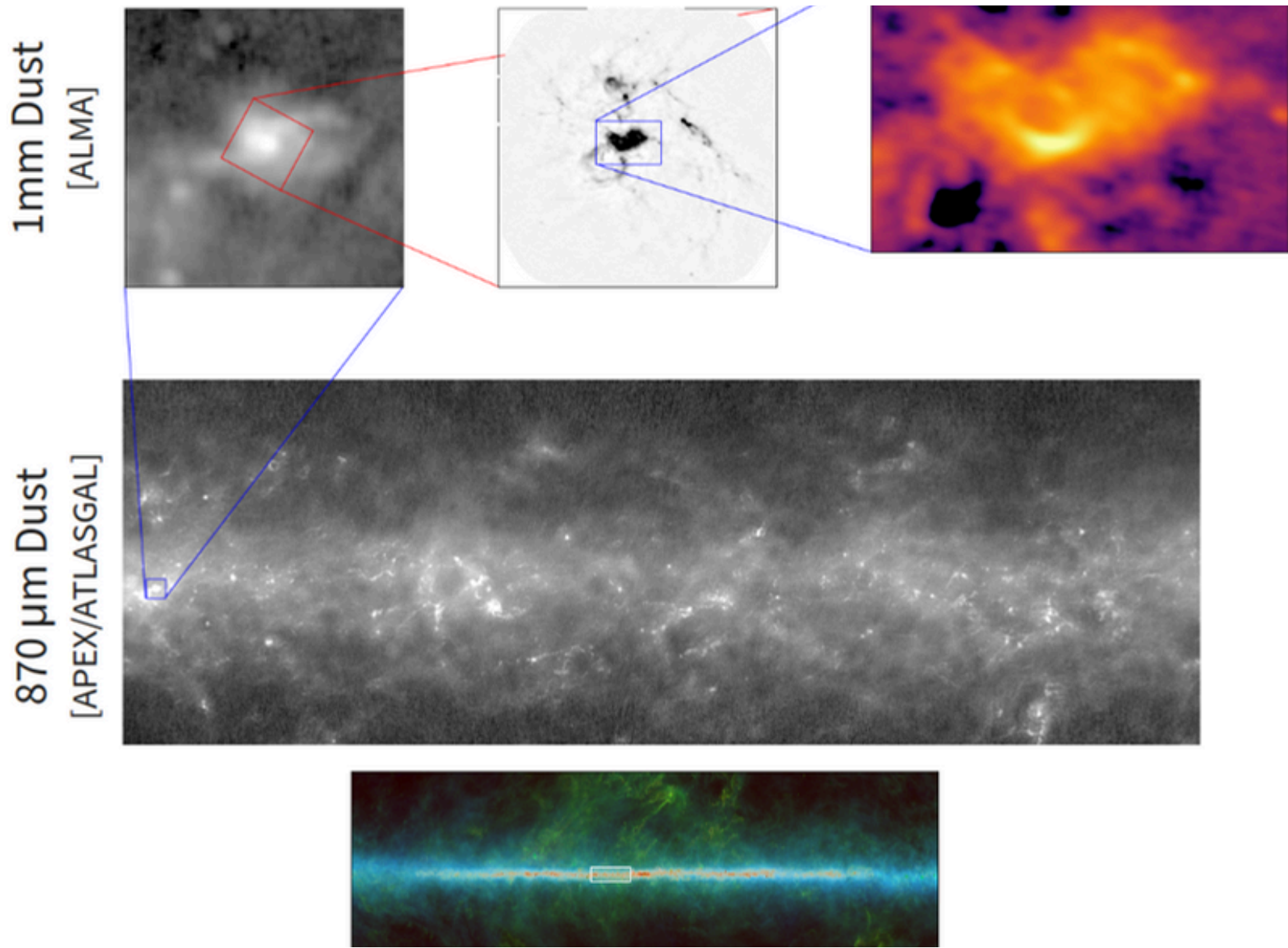
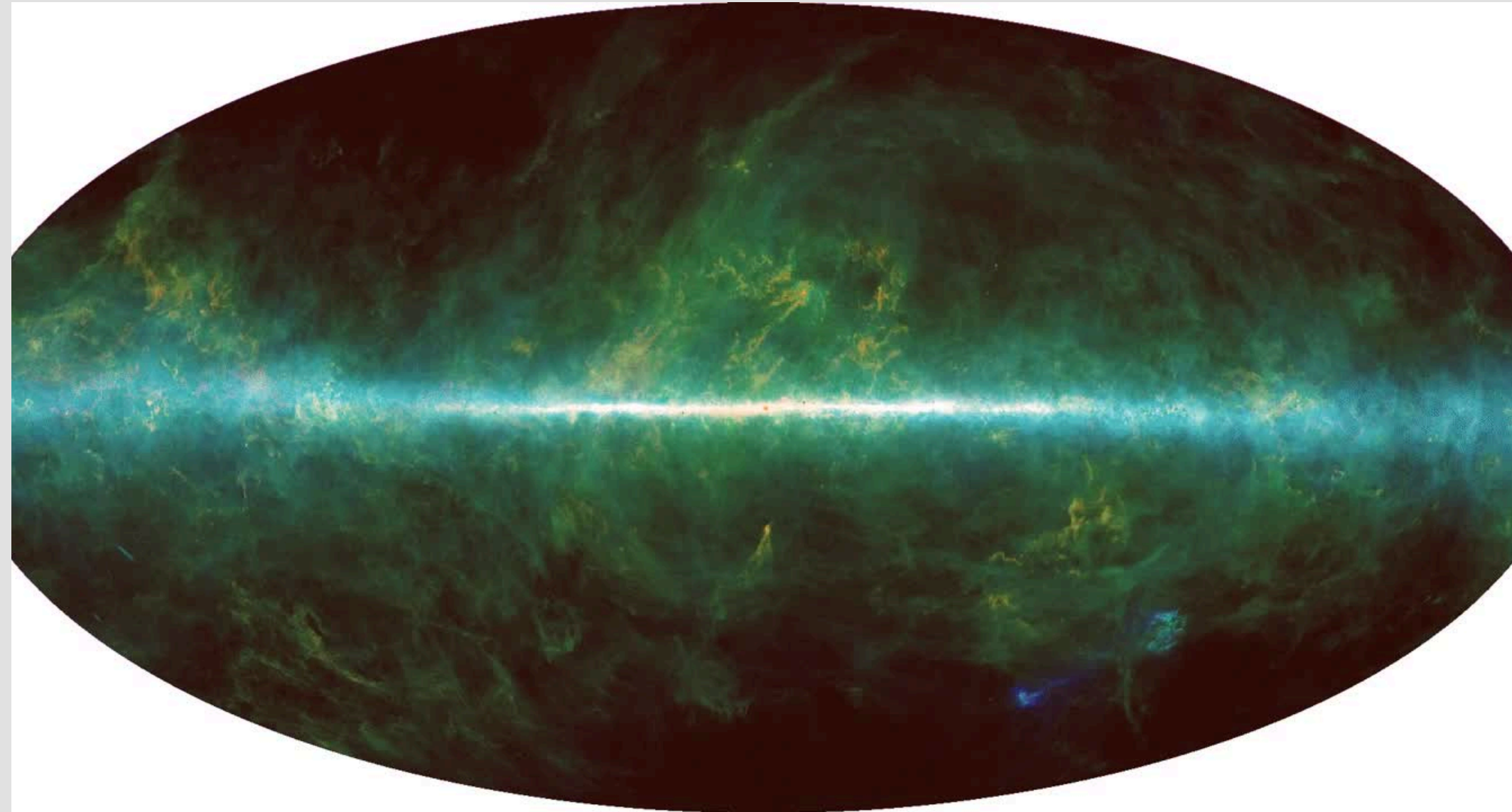


Figure 5. Ginsburg,A. (2024)



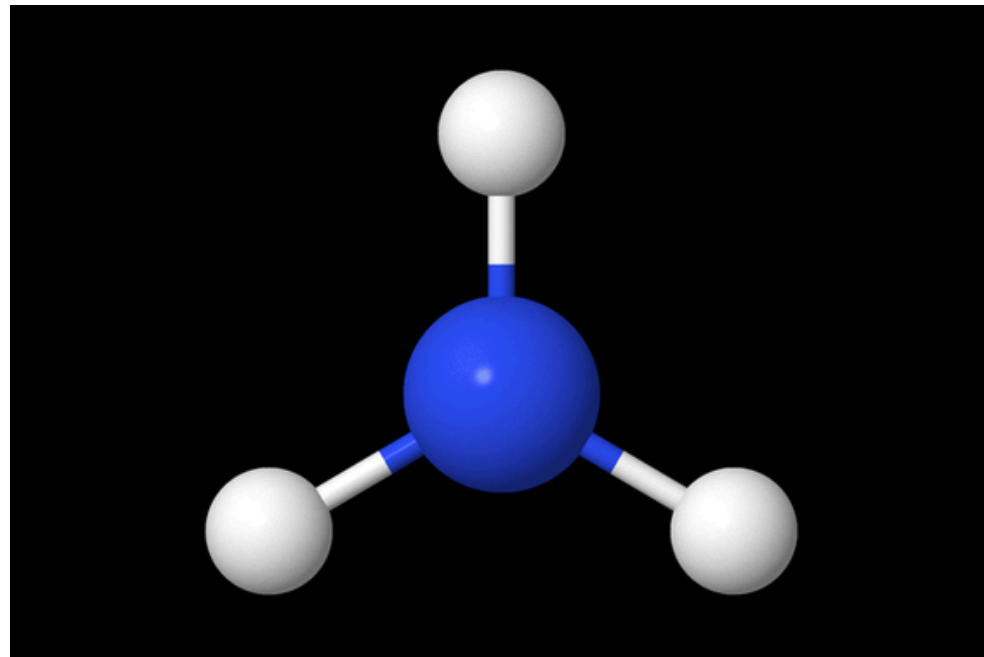
Video 1. Ginsburg,A. (2024)

MOLECULAR TRACING

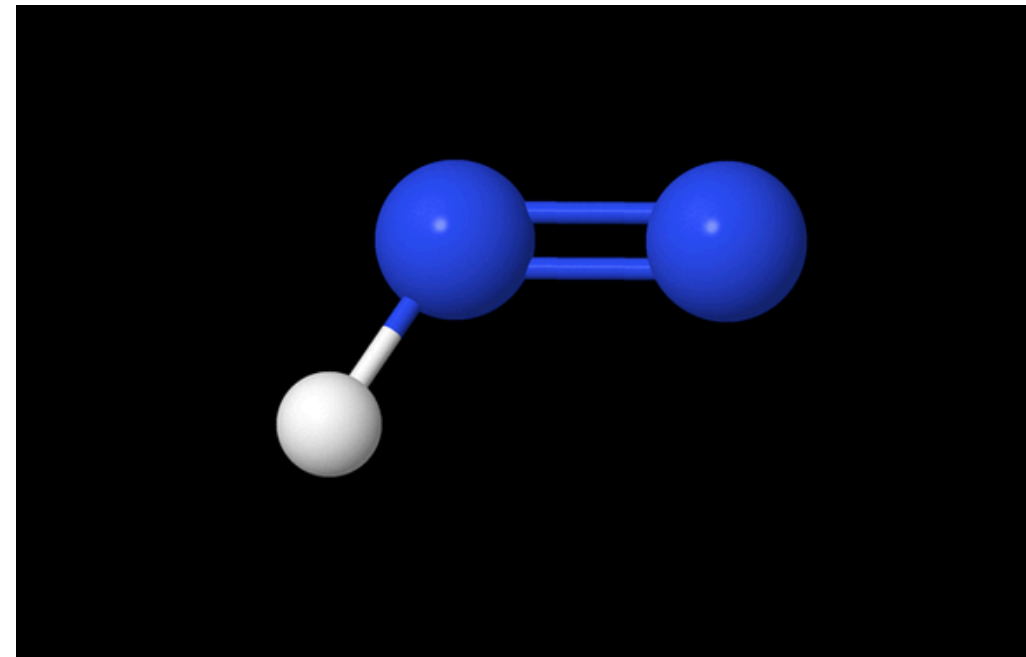
Table 1.2 Molecules found in interstellar clouds

<i>Simple neutral molecules</i>
H ₂ , CH, CN, CO, HCl, NH, NO, NS, OH, PN, SO, SiO, SiS, CS, HF, O ₂ , SH, CH ₂ , HCN, HCO, H ₂ O, H ₂ S, HNC, HNO, N ₂ O, OCS, SO ₂ , CO ₂ , NH ₂ , HO ₂ , NH ₃ , H ₂ CO, H ₂ CS, CH ₃ , H ₂ O ₂ , CH ₄
<i>Ionic species</i>
(Cation)
CH ⁺ , CO ⁺ , SO ⁺ , CF ⁺ , OH ⁺ , SH ⁺ , HCl ⁺ , ArH ⁺ , HCO ⁺ , HCS ⁺ , HOC ⁺ , N ₂ H ⁺ , H ₃ ⁺ , H ₂ O ⁺ , H ₂ Cl ⁺ , OH ₃ ⁺ , HCNH ⁺ , HCO ₂ ⁺ , C ₃ H ⁺ , H ₂ COH ⁺ , NH ₄ ⁺ , H ₂ NCO ⁺ , HC ₃ NH ⁺

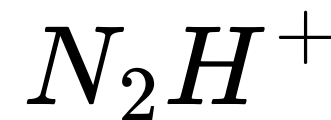
Table 1. Yamamoto, S. (2017)



Ammonia



Dyazenylum



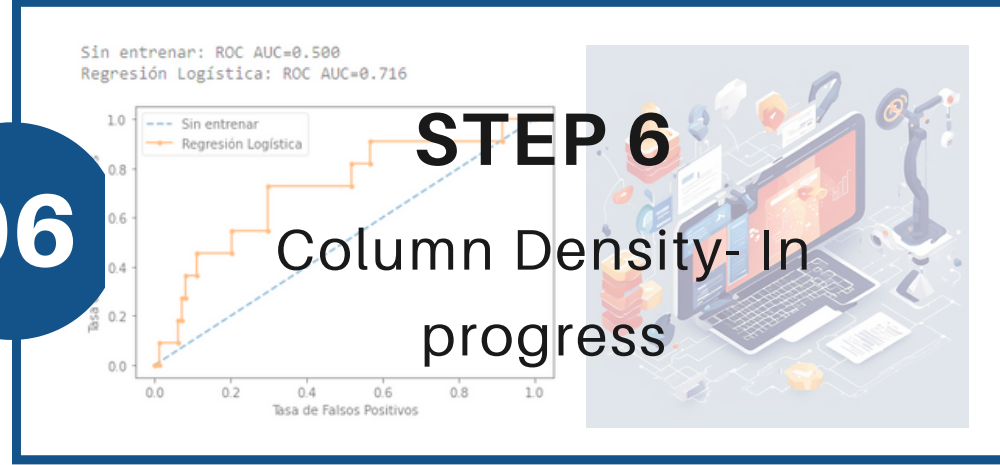
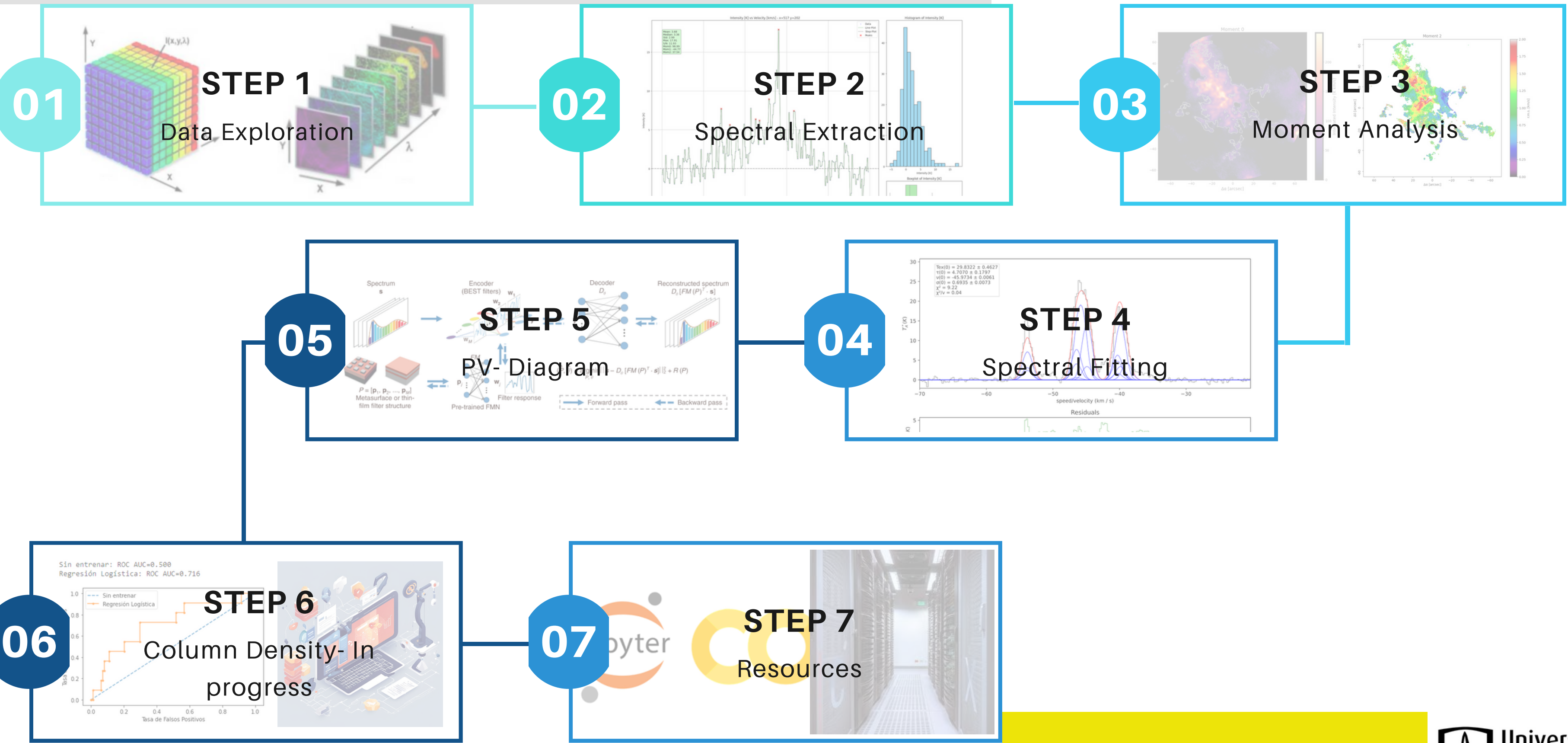
Protocluster cloud name ⁽¹⁾	RA ⁽¹⁾ [ICRS]	Dec ⁽¹⁾	V _{LSR} ⁽¹⁾ [km s ⁻¹]	d [kpc]
W51-E	19:23:44.18	+14:30:29.5	+55	5.4 ± 0.3
W43-MM1	18:47:47.00	-01:54:26.0	+97	5.5 ± 0.4
G333.60	16:22:09.36	-50:05:58.9	-47	4.2 ± 0.7
W51-IRS2	19:23:39.81	+14:31:03.5	+55	5.4 ± 0.3
G338.93	16:40:34.42	-45:41:40.6	-62	3.9 ± 1.0
G010.62	18:10:28.84	-19:55:48.3	-2	4.95 ± 0.5
W43-MM2	18:47:36.61	-02:00:51.1	+97	5.5 ± 0.4
G008.67	18:06:21.12	-21:37:16.7	+37.6	3.4 ± 0.3
G012.80	18:14:13.37	-17:55:45.2	+37	2.4 ± 0.2
G327.29	15:53:08.13	-54:37:08.6	-45	2.5 ± 0.5
W43-MM3	18:47:41.46	-02:00:27.6	+97	5.5 ± 0.4
G351.77	17:26:42.62	-36:09:20.5	-3	2.0 ± 0.7
G353.41	17:30:26.28	-34:41:49.7	-17	2.0 ± 0.7
G337.92	16:41:10.62	-47:08:02.9	-40	2.7 ± 0.7
G328.25	15:57:59.68	-53:58:00.2	-43	2.5 ± 0.5

Table 2. Motte et al. (2018)

N₂H⁺ ion is key in protocluster studies, tracing dense, cold gas in star formation areas. Resistant to freezing and stellar radiation, it reveals early-stage star formation dynamics and chemistry.

Methodology N2H+

METHODOLOGY N_2H^+



DIAZENYLUM N_2H^+

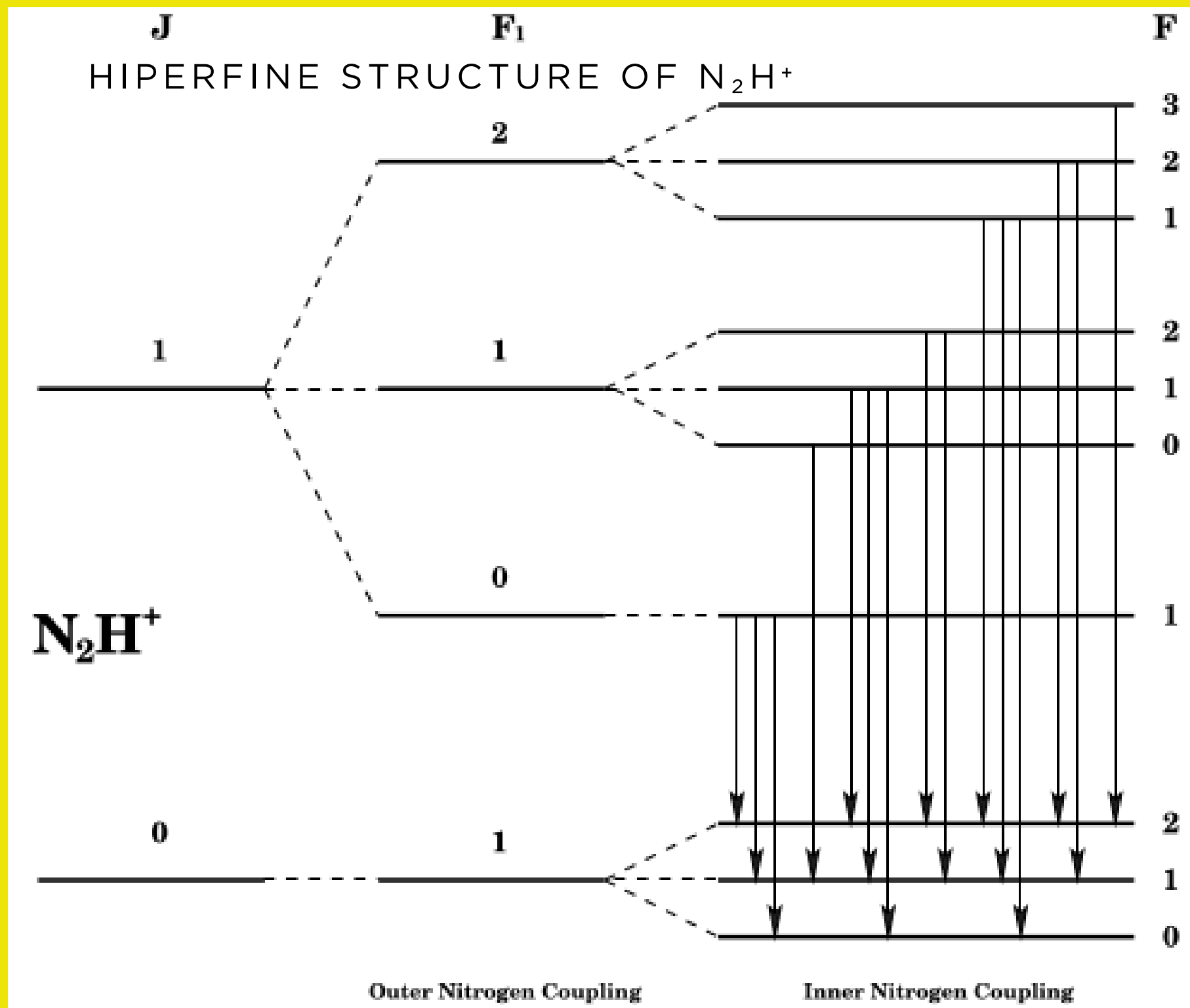


Figure 6. Caselli et al. (1995)

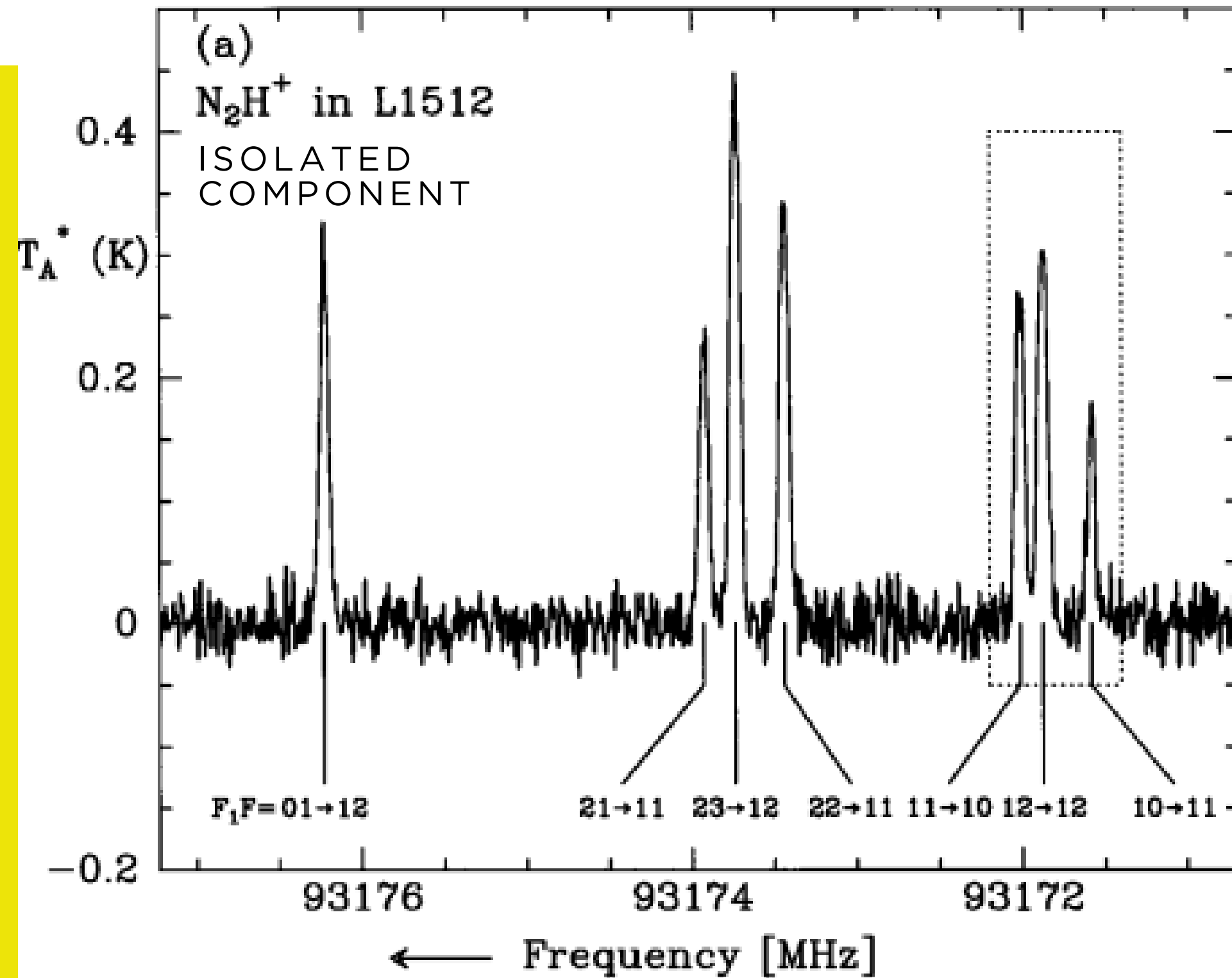


Figure 7. Caselli et al. (1995)

THE P-V DIAGRAM

Gas velocity structure of the Orion A Integral Shaped Filament

Valentina González Lobos,^{1*} Amelia M. Stutz^{1,2}

¹Departamento de Astronomía, Facultad de Ciencias Físicas y Matemáticas, Universidad de Concepción, Concepción, Chile

²Max-Planck-Institute for Astronomy, Königstuhl 17, 69117 Heidelberg, Germany

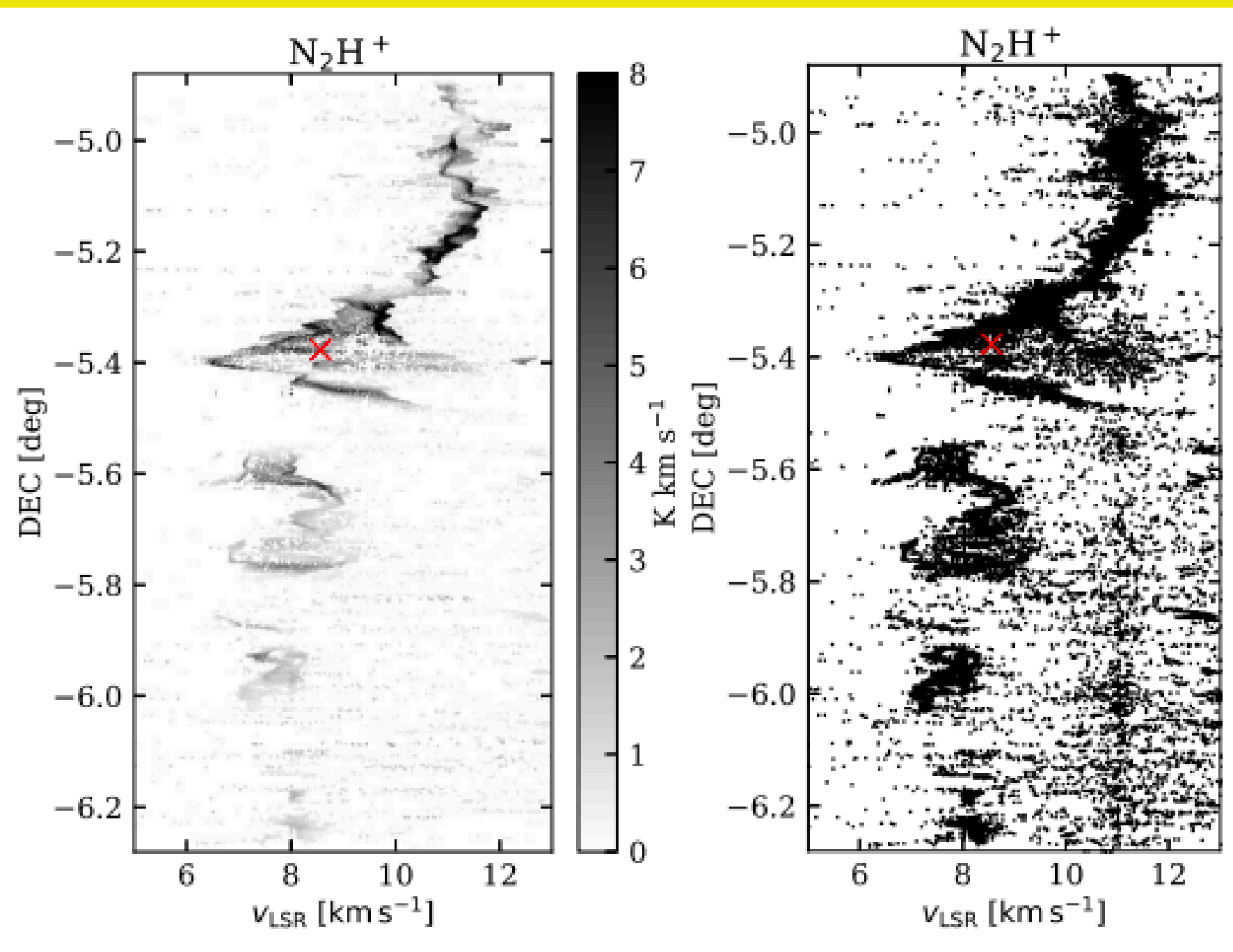


Figure 8. Lobos et al. (2019)

COLUMN DENSITY

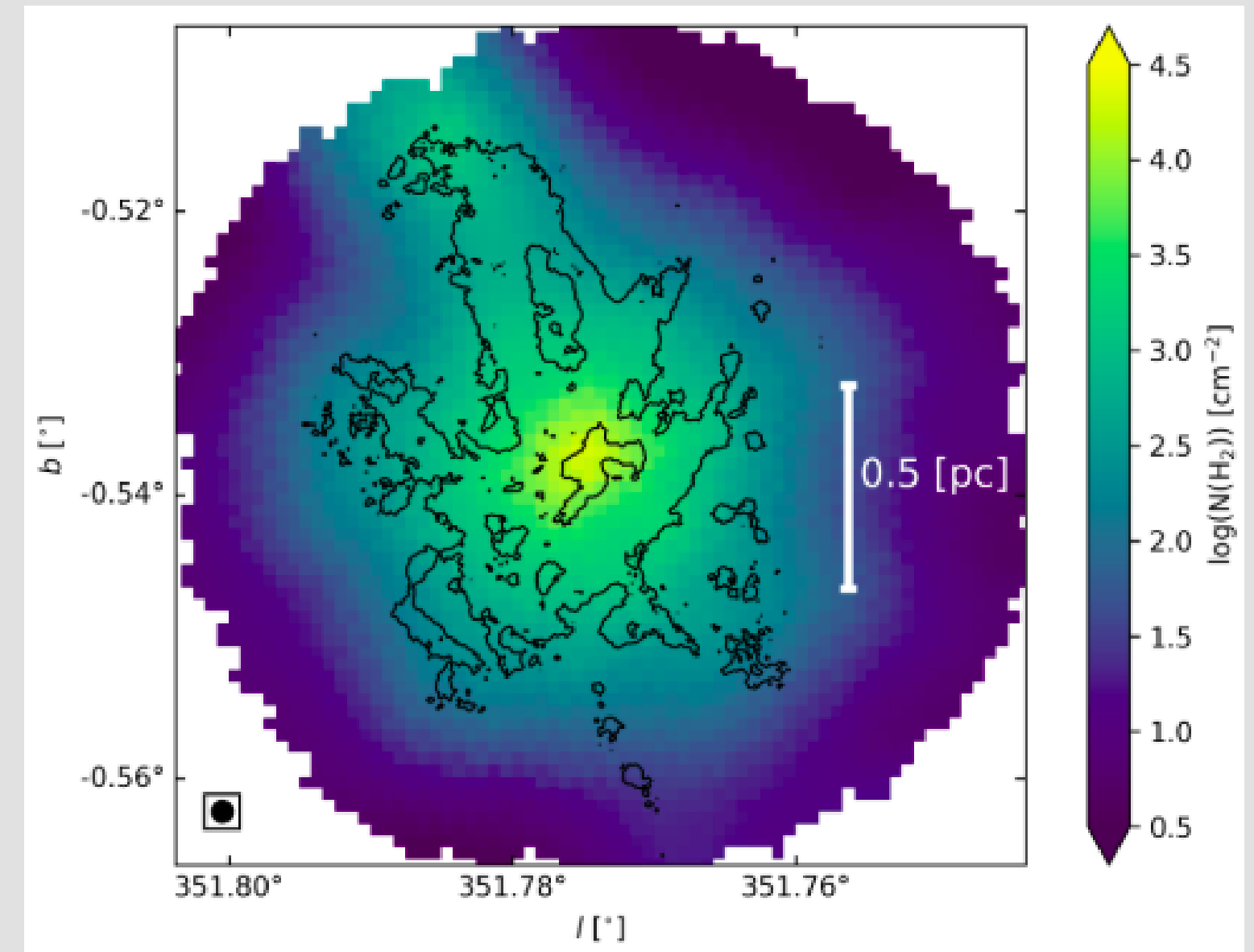


Figure 9. Garrido, N. (2024)

Filament Rotation in the California L1482 Cloud

Álvarez-Gutiérrez¹, A. M. Stutz^{1,2}, C. Y. Law^{3,4}, S. Reissl⁵, R. S. Klessen^{5,6}, N. W. C. Leigh¹,
H.-L. Liu^{1,3,8}, and R. A. Reeves¹

ONE COMPONENT SPECTRUM

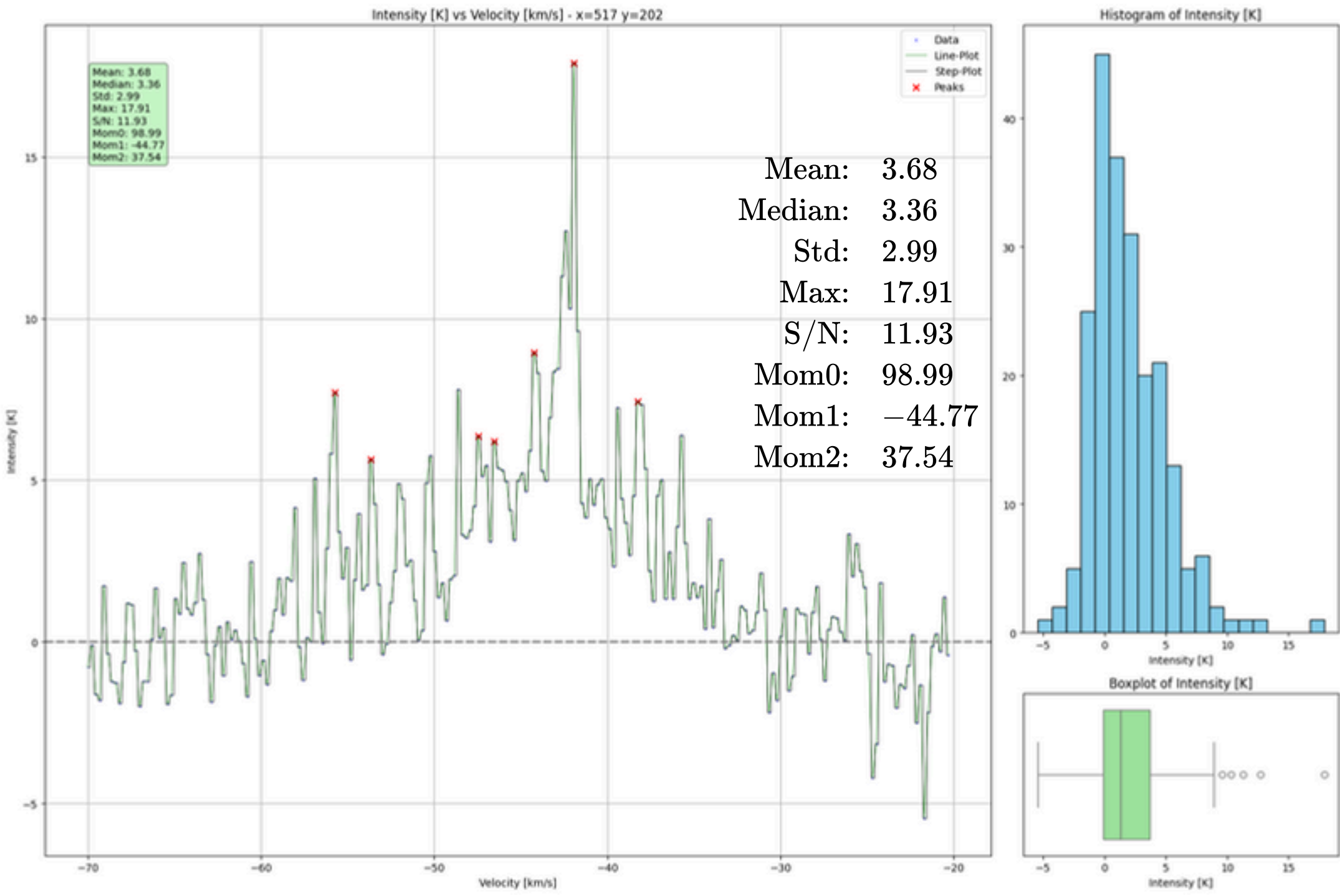
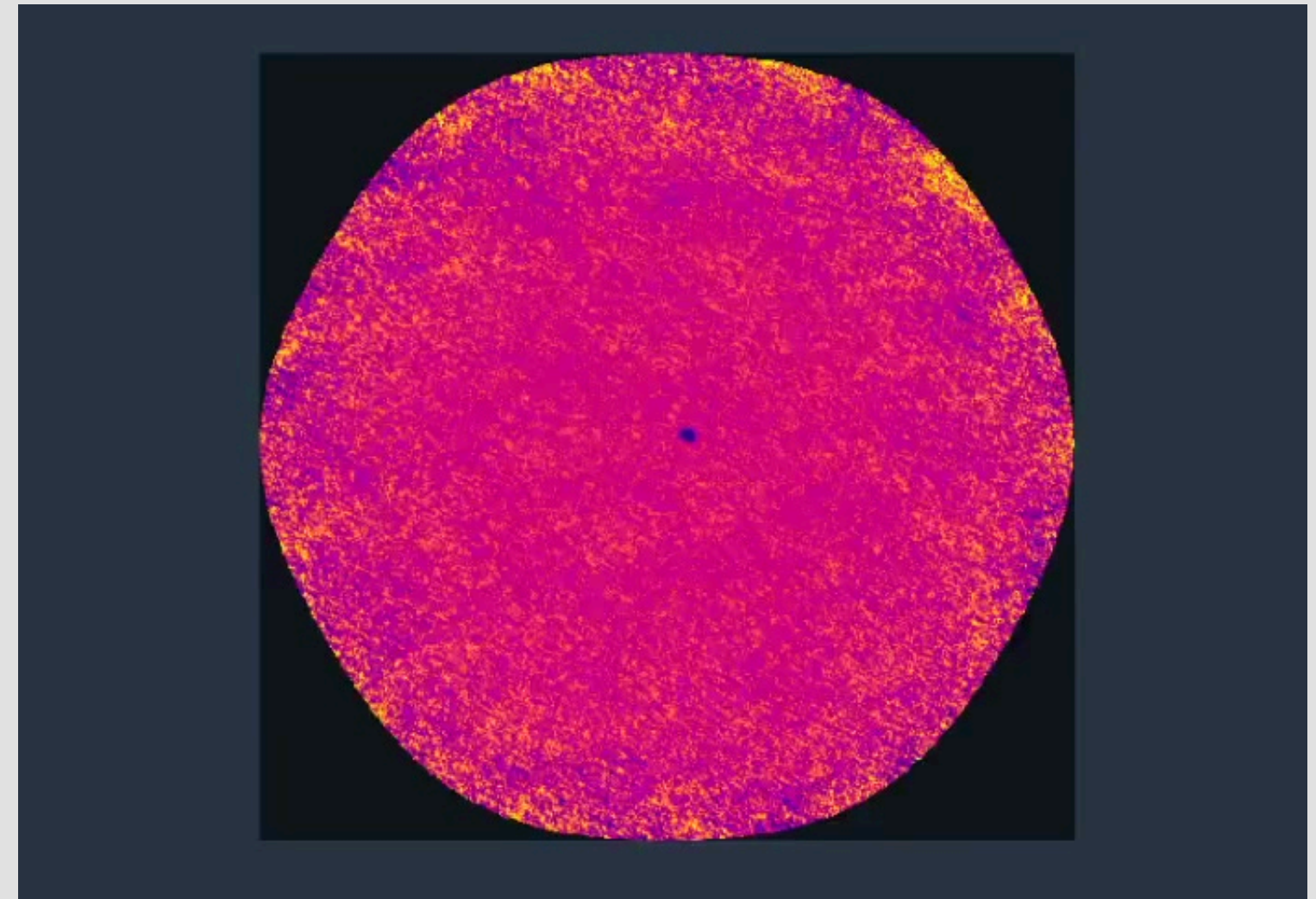


Figure 10. Spectrum for one component



Video 3. Spectral Axis

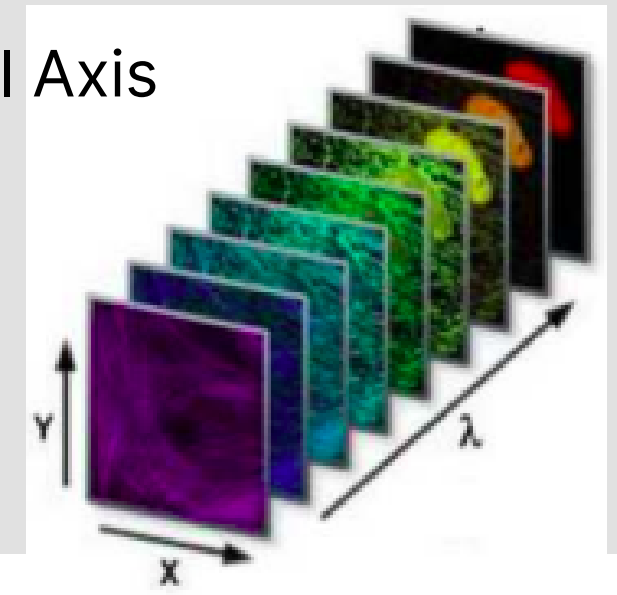
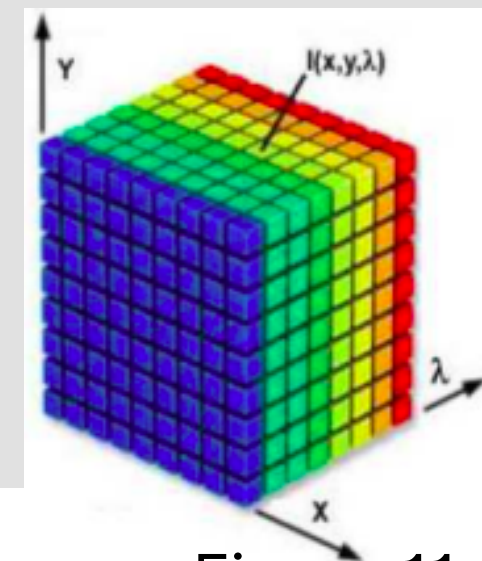


Figure 11. Data Cube. Ibraheem , I. (2015).

MOMENTUM ANALYSIS

$$M_0 = \sum_i T_B^*(v_i) \Delta v$$

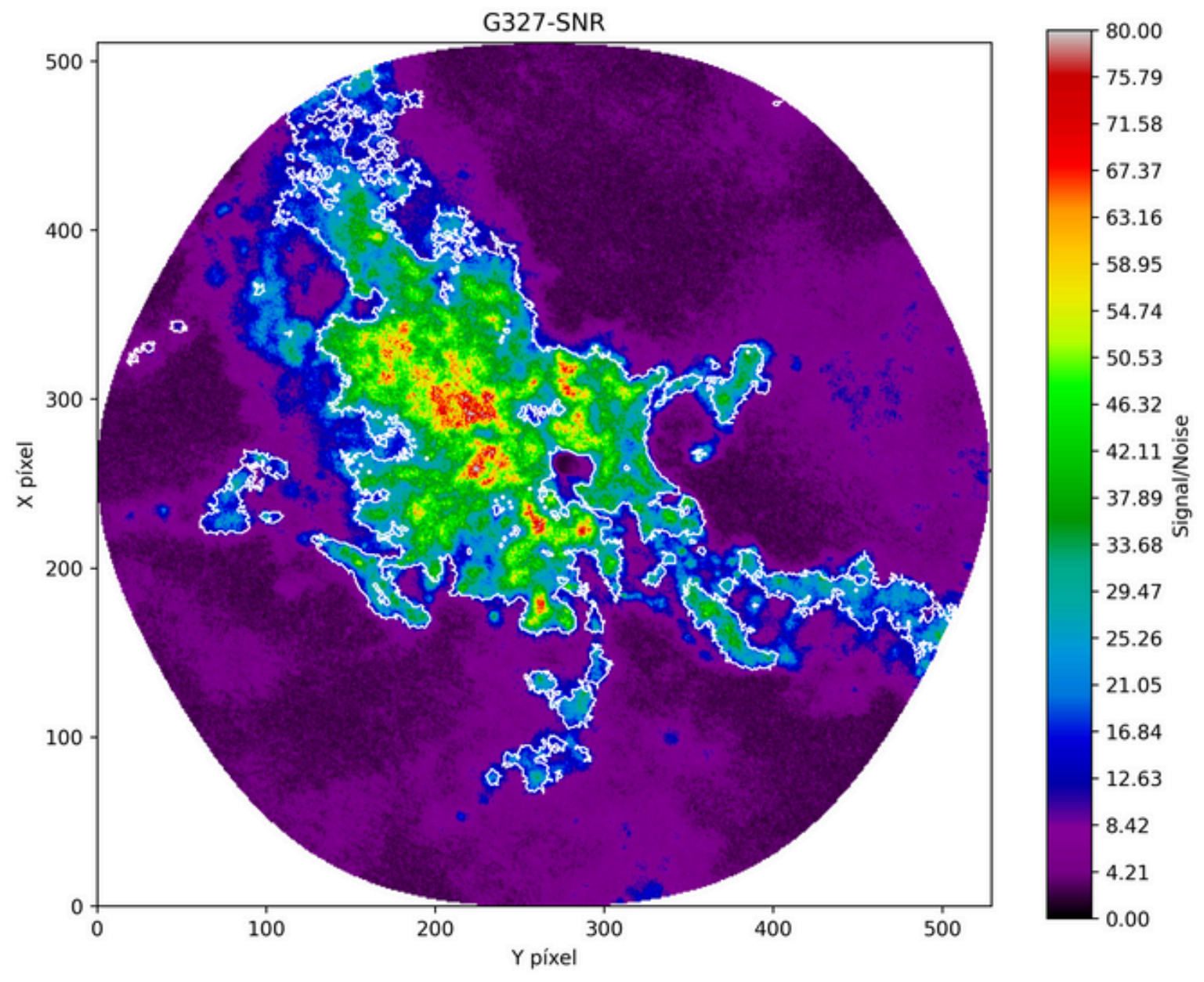
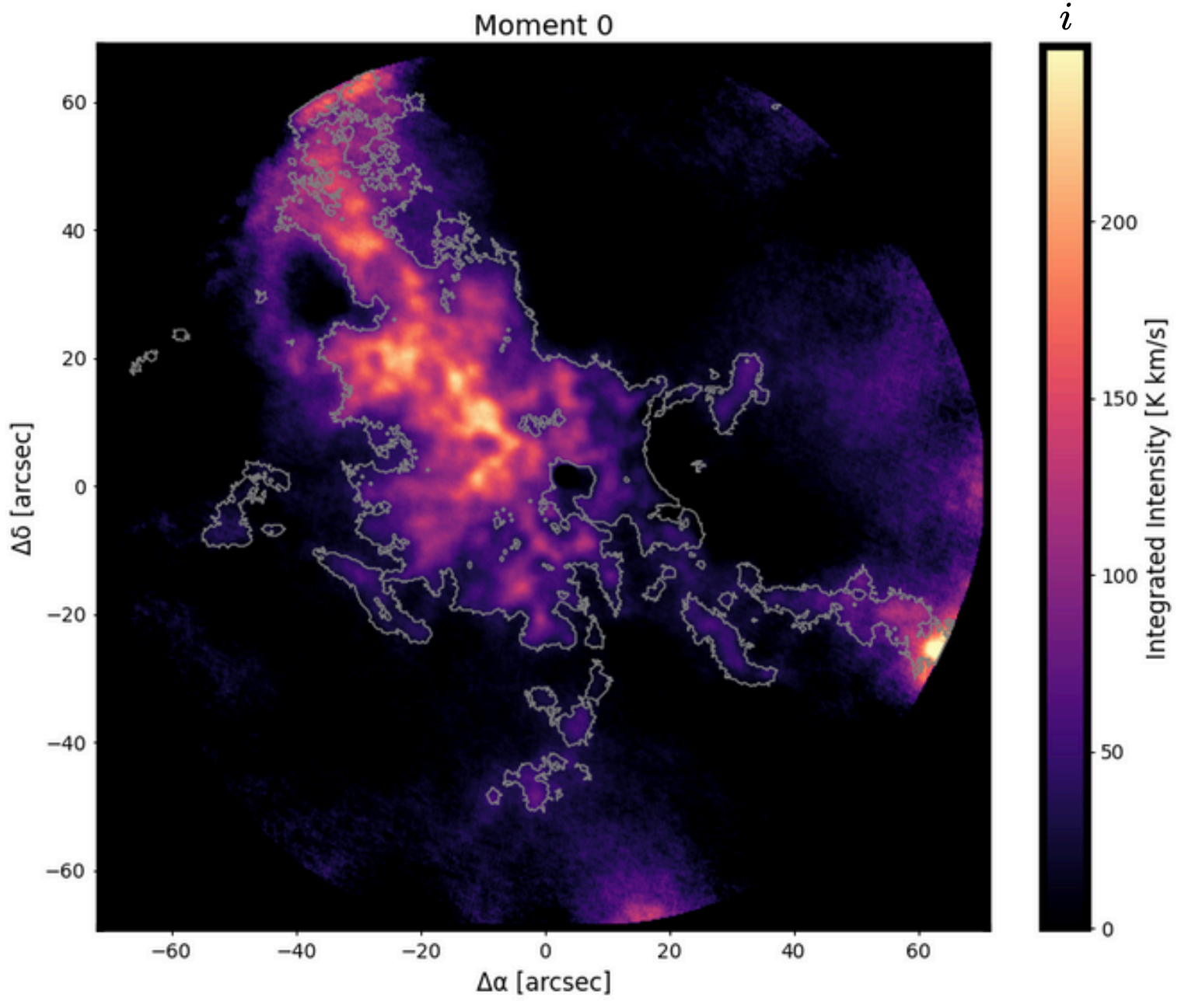


Figure 12. Moment Zero

Figure 13. Signal to Noise

MOMENTUM ANALYSIS II

$$M_1 = \frac{\sum_i T_B^*(v_i) v_i \Delta v}{\sum_i T_B^*(v_i) \Delta v}$$

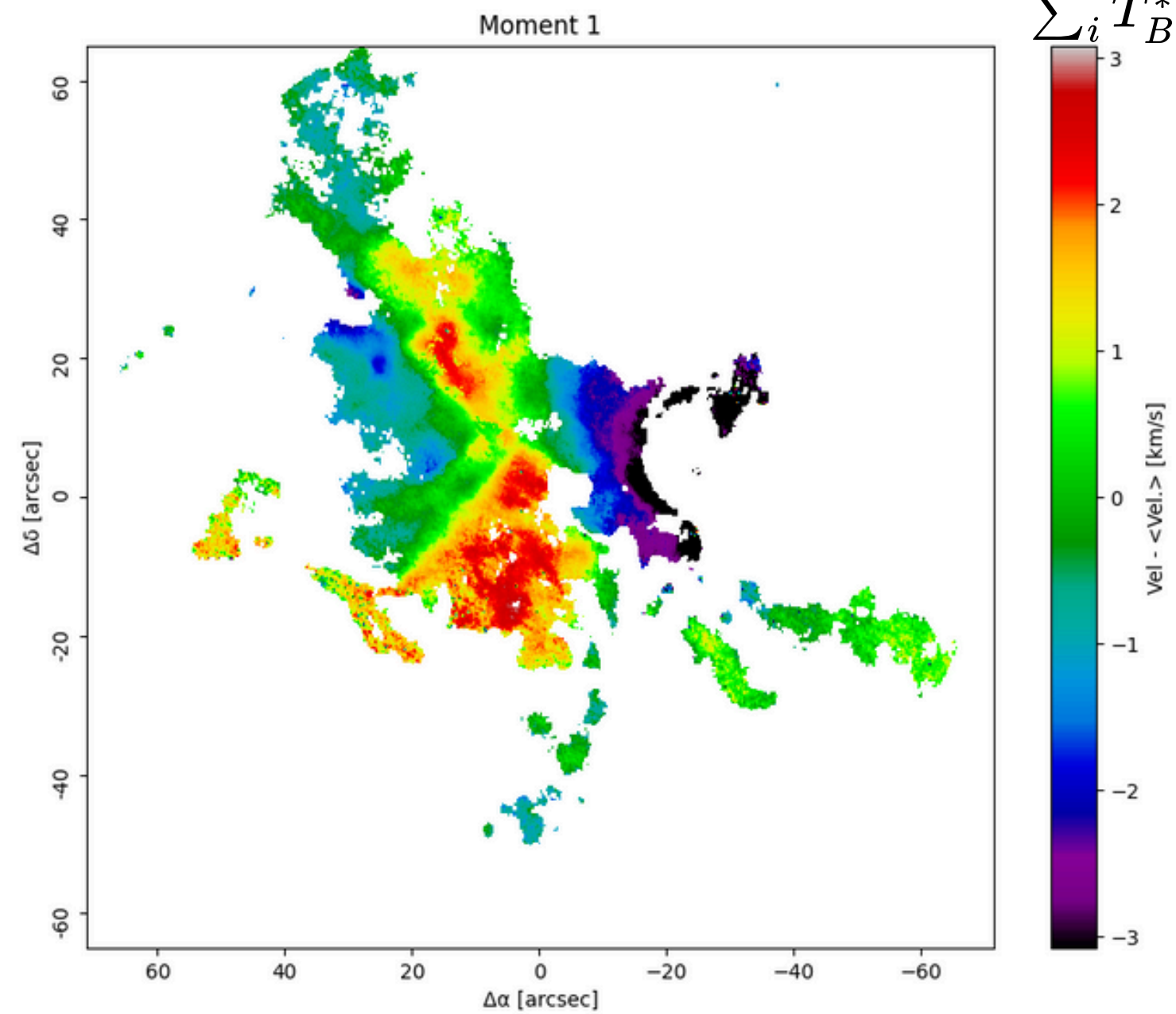


Figure 14. Moment One

$$M_2 = \sqrt{\frac{\sum_i T_B^*(v_i) (v_i - M_1)^2 \Delta v}{\sum_i T_B^*(v_i) \Delta v}}$$

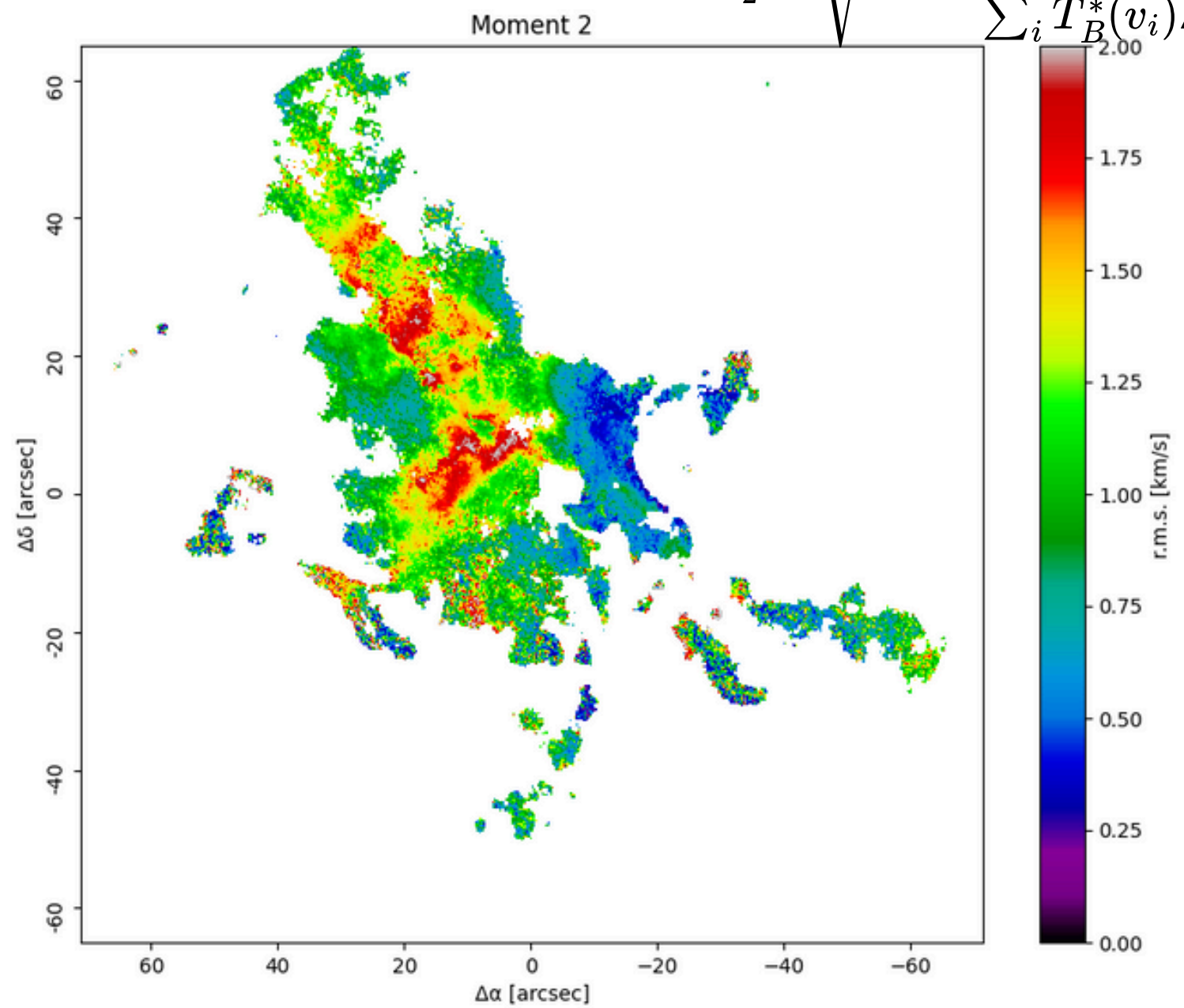


Figure 15. Moment Two

FIT ONE COMPONENT

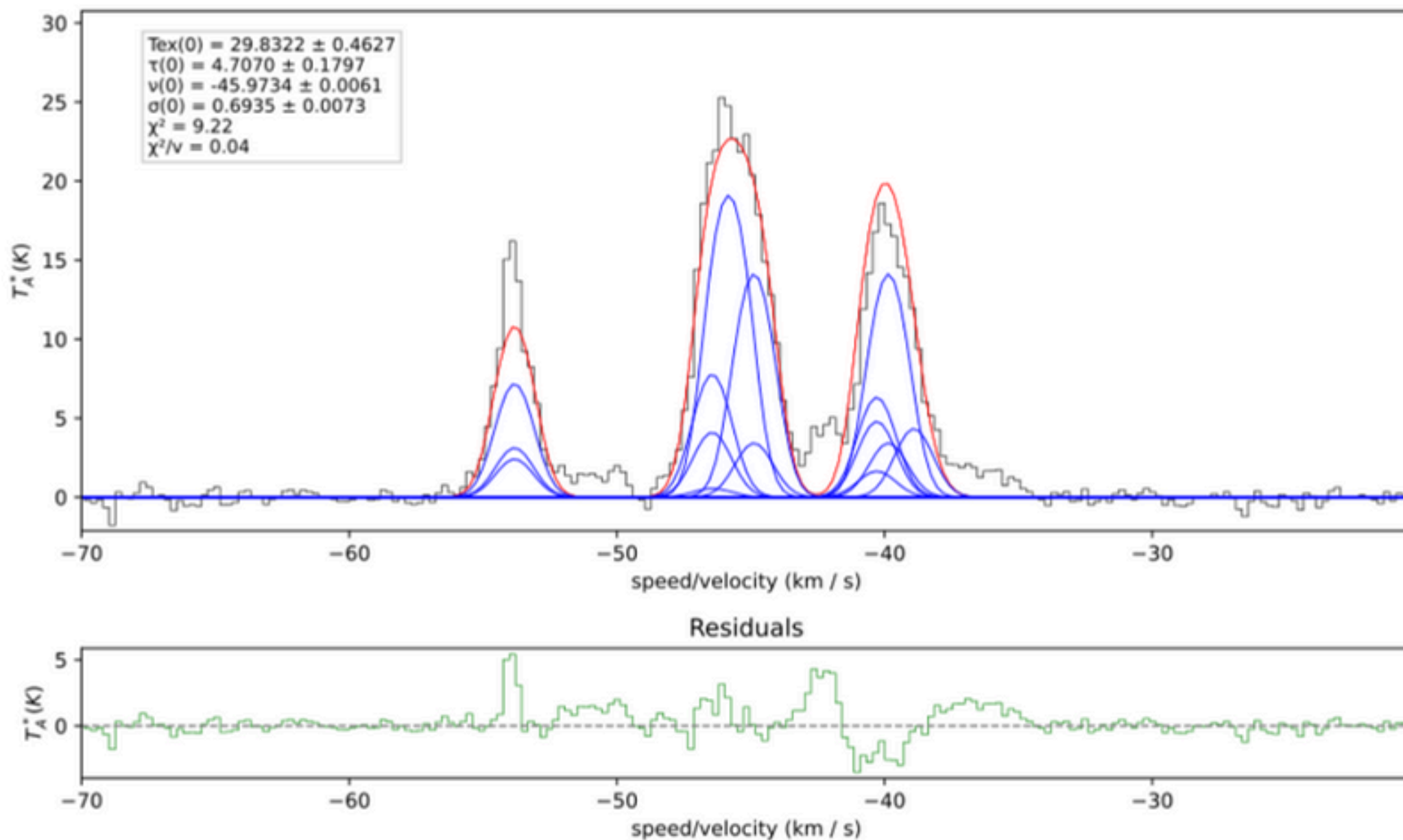


Figure 16. Fit Spectrum

$$T_{\text{ex}}(0) = 29.8322 \pm 0.4627$$

$$\tau(0) = 4.7070 \pm 0.1797$$

$$v_{\text{rms}}(0) = -45.9734 \pm 0.0061$$

$$\sigma(0) = 0.6935 \pm 0.0073$$

$$\chi^2 = 9.22$$

$$\chi^2/\nu = 0.04$$

FIT DATA CUBE

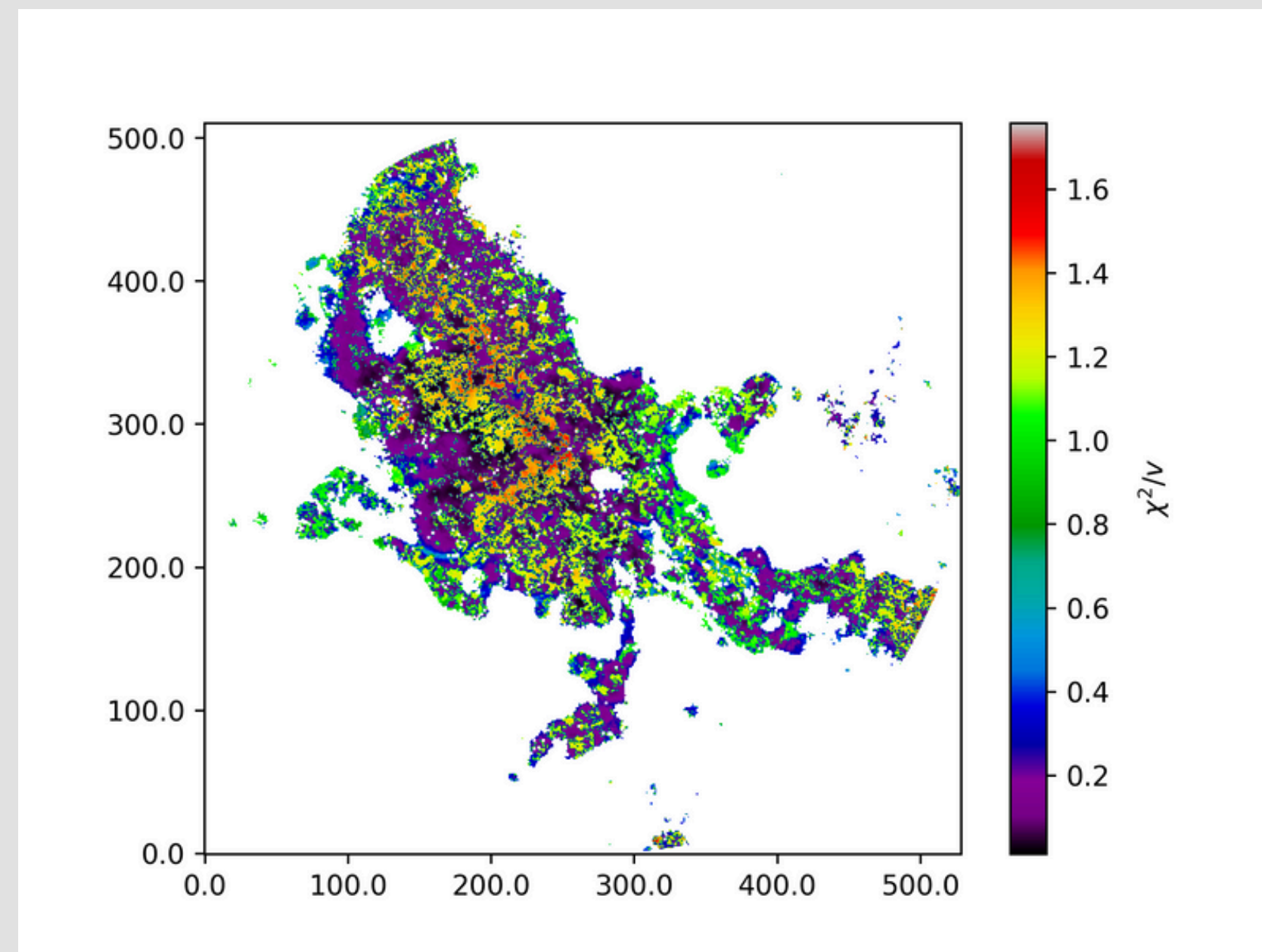


Figure 17. Chi Square

MWYDYN

SDC326_n2h+_TP+7m+12m.subcube.fits
snrlim=10.0 delbic=20.0

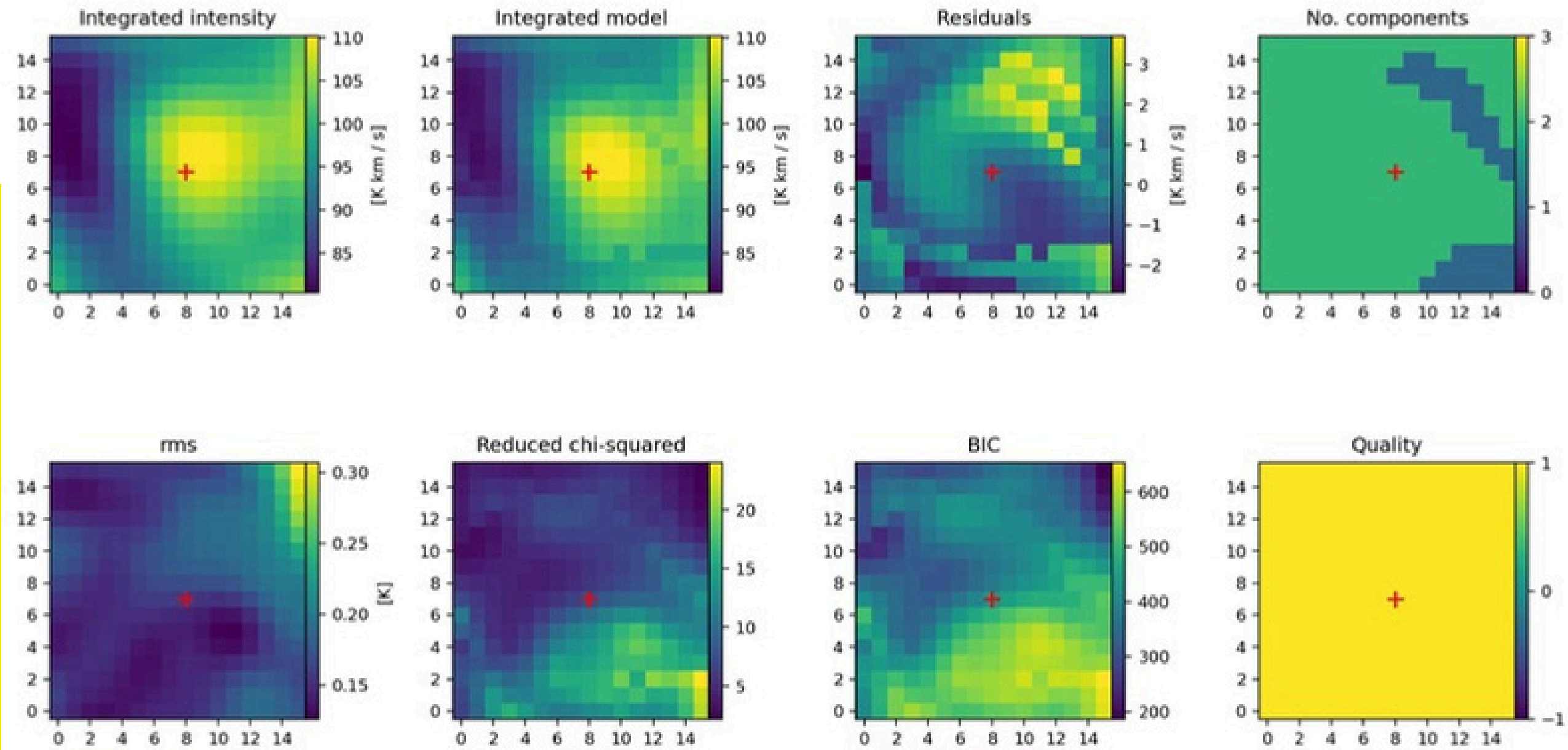
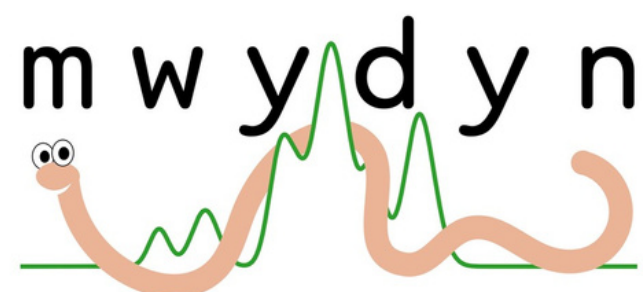


Figure 18. Summary of MWYDYN



The Bayesian Information Criterion (BIC) is a metric used for model selection in statistics and machine learning that balances model fit quality with model complexity.

FIT TWO COMPONENT

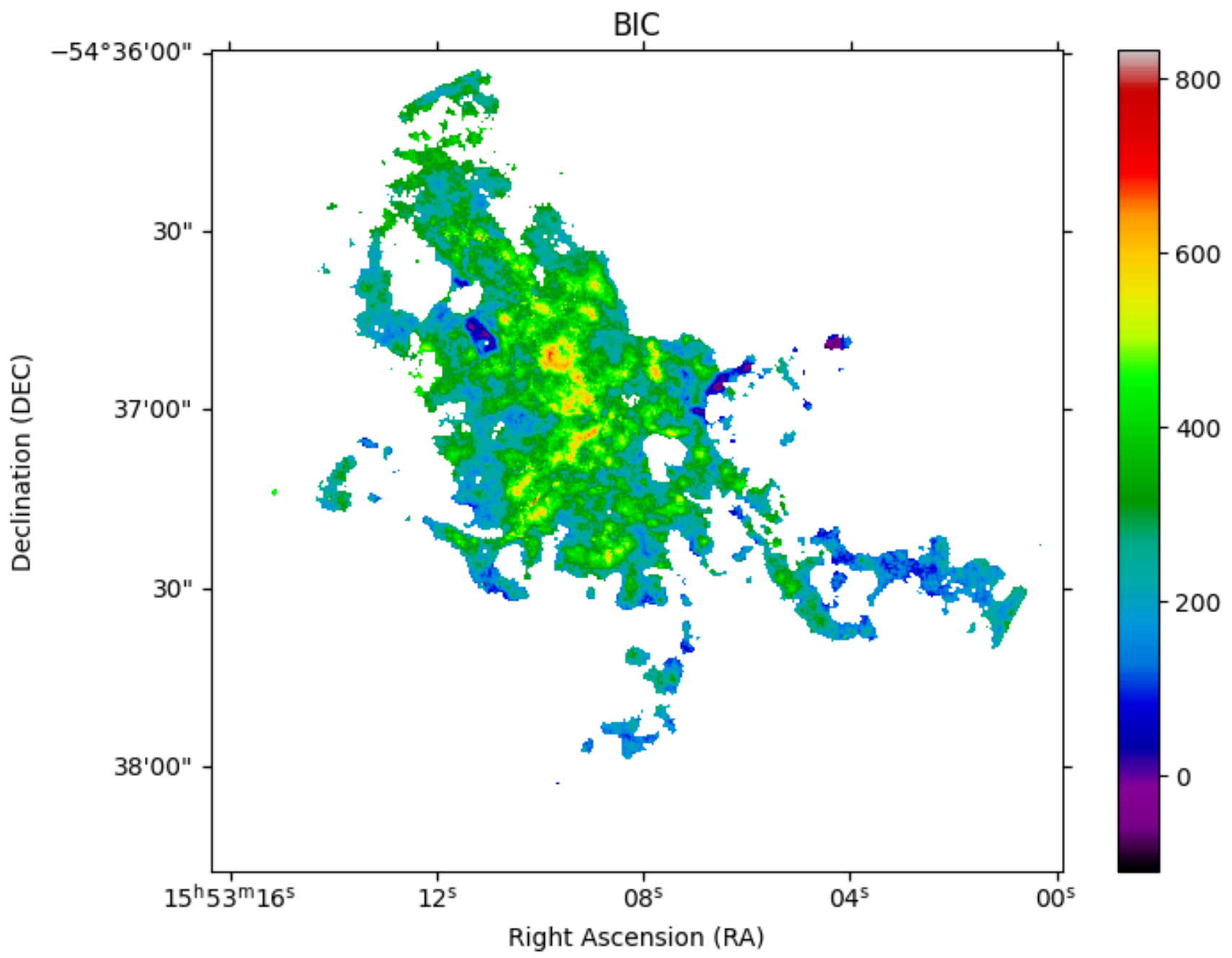


Figure 19. BIC

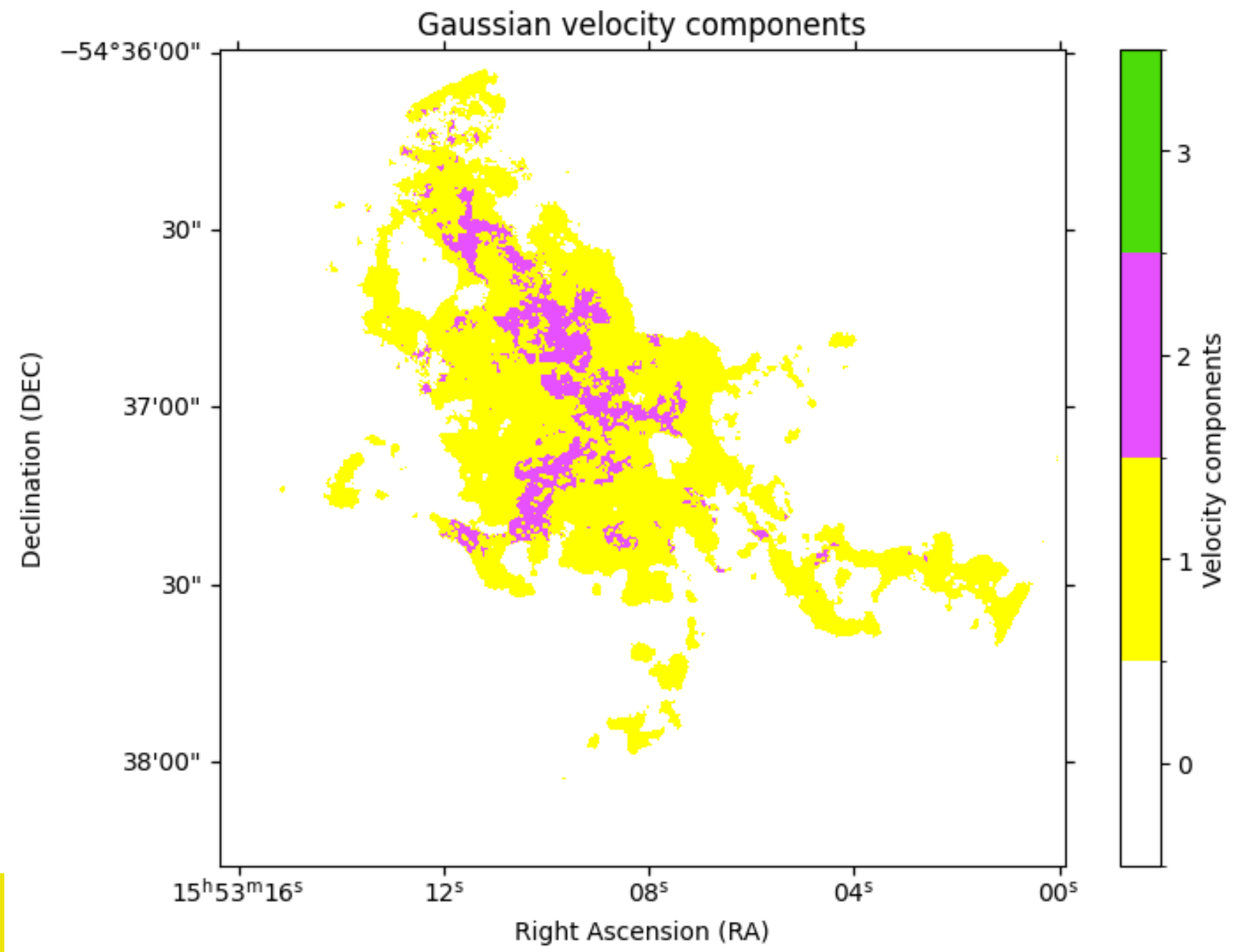


Figure 20. Two Velocity Components

P-V DIAGRAM

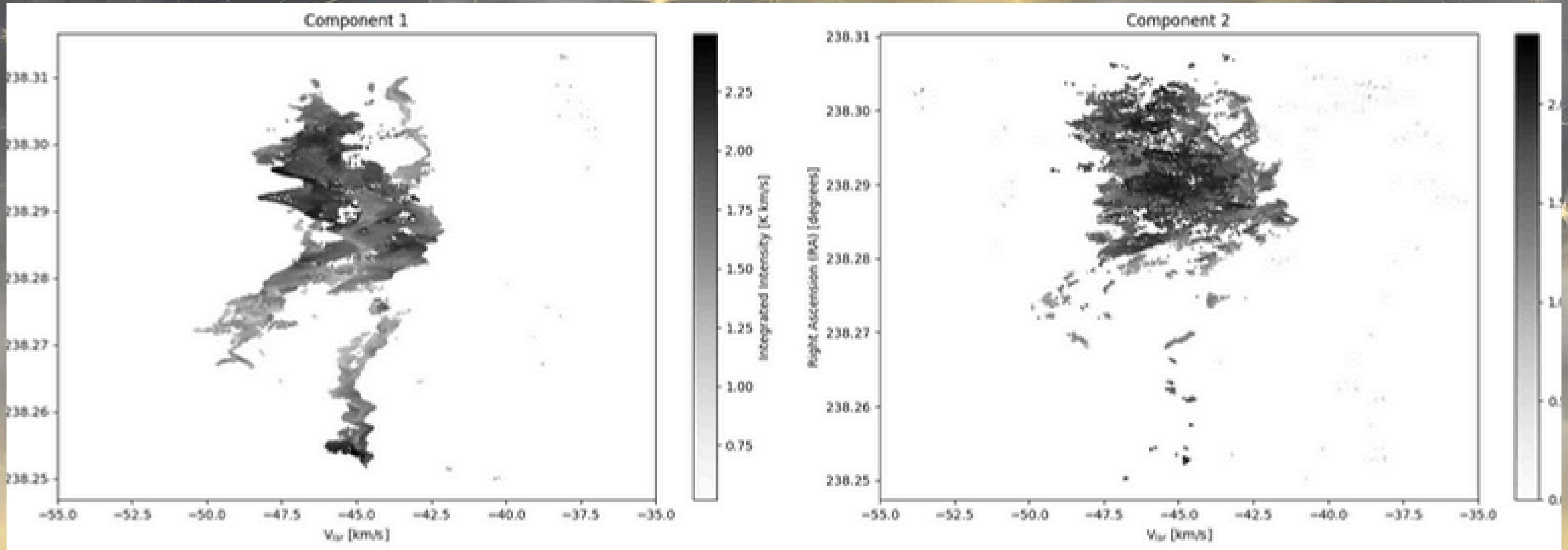


Figure 21. P-V Diagram one and two components of N₂H⁺

VELOCITY DISTRIBUTION

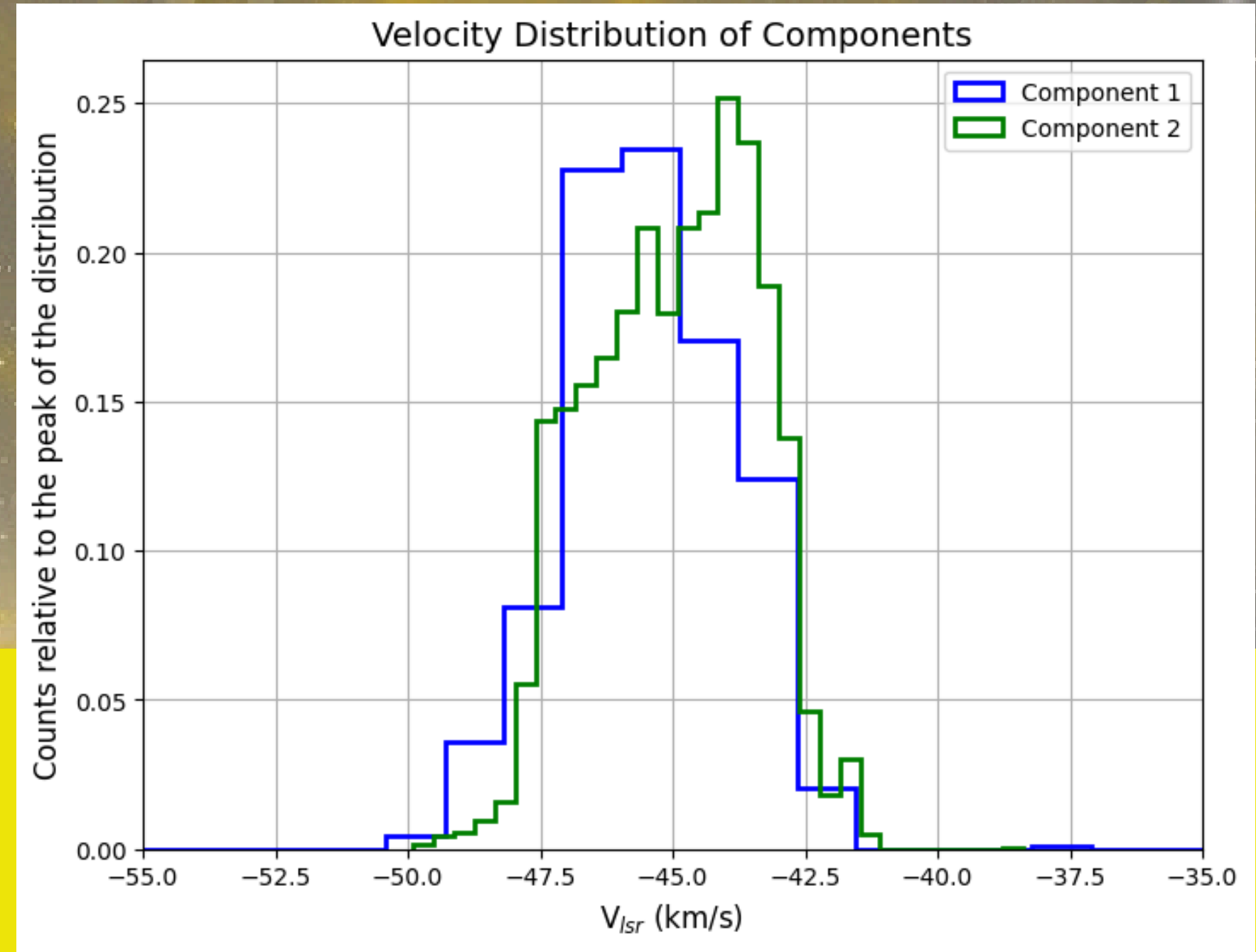
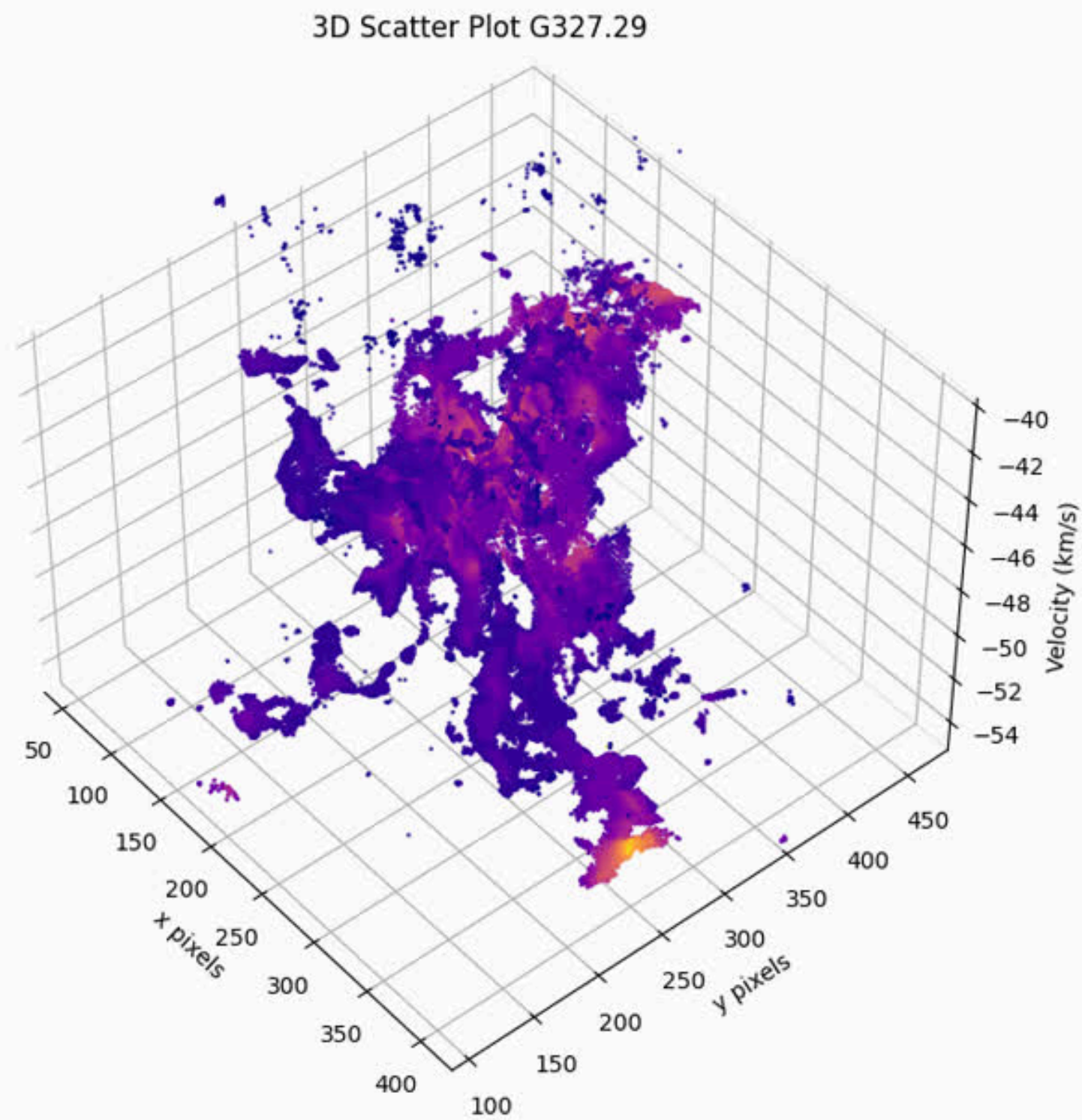


Figure 22. Distributions of components of N₂H⁺

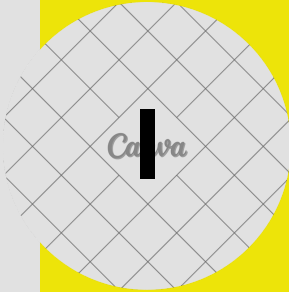
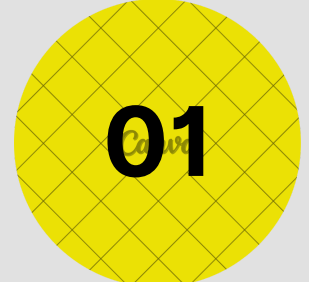
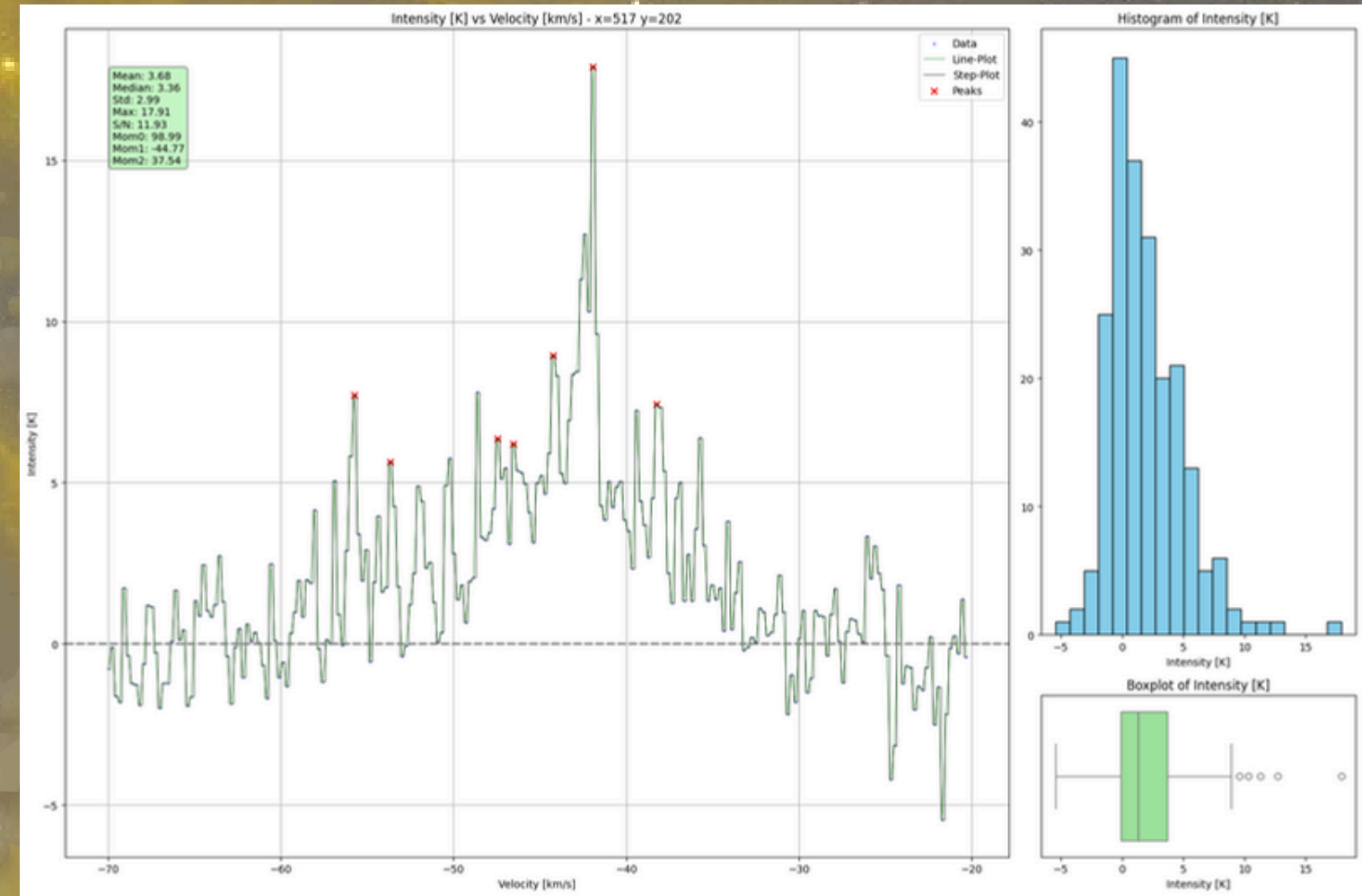
Conclusions

Conclusions

The gas in G327.29 is concentrated in dense structures, traced effectively using N_2H^+ , ideal for early star formation studies.

Velocity analysis shows multiple components, indicating dynamic interactions like gravitational collapse and accretion flows.

Bayesian models helped identify key gas motions, such as turbulence, shaping massive star formation.



Use an autoencoder to extract the physical parameters of the cloud, enabling a more efficient and detailed analysis of the data.

Compare N_2H^+ observations with other molecular tracers, such as NH_3 or CO , to validate and complement the findings.

Complete a comprehensive morphological analysis of N_2H^+ to better understand its role in early star formation.

THANK YOU
SO MUCH!

Presentation by **Fredy Orjuela**
Universidad de los Andes | Physics Department | 2024

THE
END

REFERENCES

- Ward-Thompson, D., & Whitworth, A. P. (2011). An introduction to star formation. Cambridge University Press.
- Purcell, C. (2006). What's in the brew? A study of the molecular environment of methanol masers and UCHII regions (Doctoral dissertation, UNSW Sydney).
- Kroupa, P. (2001). On the variation of the initial mass function. *Monthly Notices of the Royal Astronomical Society*, 322(2), 231-246.
- Pannuti, T. G. (2020). The physical processes and observing techniques of radio astronomy. Editorial: Springer.
- Yamamoto, S. (2017). Introduction to astrochemistry. Editorial: Springer, 614.
- Motte, F., Bontemps, S., & Louvet, F. (2018). High-mass star and massive cluster formation in the milky way. *Annual Review of Astronomy and Astrophysics*, 56, 41-82.
- Caselli, P., Myers, P. C., & Thaddeus, P. (1995). Radio-astronomical spectroscopy of the hyperfine structure of N₂H⁺. *the Astrophysical Journal*, 455(1), L77.
- Matsumoto, K., Camps, P., Baes, M., De Ceuster, F., Wada, K., Nakagawa, T., & Nagamine, K. (2023). Self-consistent dust and non-LTE line radiative transfer with SKIRT. *Astronomy & Astrophysics*, 678, A175.
- Dullemond, C. P. (2012). *RADMC-3D: A multi-purpose radiative transfer tool*. Retrieved from <https://www.ita.uni-heidelberg.de/~dullemond/software/radmc-3d/radmc3d.pdf>
- González Lobos, V., & Stutz, A. M. (2019). Gas velocity structure of the Orion A integral-shaped filament. *Monthly Notices of the Royal Astronomical Society*, 489(4), 4771-4782.
- Sandoval Garrido, N. A. (2024). Dense gas kinematics in the massive G351. 77 protocluster ALMA-IMF Large Program observations of N₂H⁺.
- Vieira, R. G., Carciofi, A. C., & Bjorkman, J. E. (2015). The pseudo-photosphere model for the continuum emission of gaseous discs. *Monthly Notices of the Royal Astronomical Society*, 454(2), 2107-2119.